UNIVERSITY OF GHANA

COLLEGE OF BASIC AND APPLIED SCIENCE

QUALITY CONTROL AND DOSIMETRY OF A WOODEN COUCH TOP FOR MEGAVOLTAGE EXTERNAL BEAM RADIOTHERAPY.

BY

HANSON JUSTICE

(10506948)

THIS THESIS IS SUBMITTED TO THE UNIERSITY OF GHANA, LEGON IN PARTIAL FULFILMENT OF THE REQUIREMENT FOR THE AWARD OF MASTER OF PHILOSOPHY IN MEDICAL PHYSICS DEGREE

DEPARTMENT OF MEDICAL PHYSICS
GRADUATE SCHOOL OF NUCLEAR AND ALLIED SCIENCES

JULY, 2016

DECLARATION

I hereby declare that apart from references made to other authors' work which have been duly acknowledge, this thesis has been the result of my own work carried out in the Department of Medical physics under the supervision of Prof. Cyril Schandorf, Dr. Francis Hasford and Mr. Samuel Nii Adu Tagoe and has not been presented for another degree.

…… Date……..

HANSON JUSTICE:
(STUDENT)

…… Date……..

PROF. CYRIL SCHANDORF

(PRINCIPAL SUPERVISOR)

…….. Date……..

DR. FRANCIS HASFORD

(CO-SUPERVISOR)

…….. Date……..

MR. SAMUEL N.A. TAGOE

(CO-SUPERVISOR)

ABSTRACT

The purpose of this study was to determine an appropriate locally fabricated wood sample that could be used to replace the wire mesh incorporated at the treatment area of EBRT couch top to circumvent dose discrepancies associated with the sagging effect of the wire mesh as a result of prolonged use. Linear attenuation coefficient and transmission factor were determined at three stipulated field sizes (5cm x 5cm, 10cm x 10cm,15cm x 15cm) and two treatment depths of 0.5cm and 5cm for five (5) wood species with each consisting of six (6) square slabs of 2.5cm thickness each. It was observed that for a particular depth, linear attenuation coefficient generally decreases as the field size increases whilst transmission factor was vice-versa. *Triplochiton scleroxylon* had the lowest average linear attenuation coefficient across the three field size as $0.0248cm^{-1}$ at a depth of 0.5cm This was followed by *Terminalia superba* of $0.0312cm^{-1}$ and that of *Albizia zygia* , *Entandrophragma candollei* and *Nesogogordonia papaverifera* were $0.0353cm^{-1}$, $0.0410cm^{-1}$ and $0.0563cm^{-1}$ respectively at the same depth. The percentage deviation in the order as arranged above were 3.6%, 3.8%, 4.5%, 2.4% and 3.9% respectively. There was the same trend (decrease μ as Fs increases) at a depth of 5cm. However, transmission factor for all the wood species increases with increased in field size with *Terminalia superba* recording a highest average TF as 0.981 and 0.952 followed by *Triplochiton scleroxylon* as 0.979 and 0.947 at a depth of 0.5cm and 5cm respectively. *Triplochiton scleroxylon* of about 2cm thickness could serve as a more affordable material to be used to replace the wire mesh.

DEDICATION

I dedicate this work to my mother Mrs. Elizabeth .A. Kaku, siblings, all radiation therapist and Medical physicist at the Korle-Bu Radiotherapy centre and to my late father; Mr. Godwyll Ahenesie Hanson; your memories will never be forgotten.

ACKNOWLEDGEMENTS

My first and foremost thanks goes to my Lord and Saviour Jesus Christ for His grace and mercies granted unto me throughout this work and to my life in general.

I am particularly grateful for immeasurable efforts of my supervisors, Prof. Cyril Schandorf, Dr. Francis Hasford and Mr. Samuel Nii Adu Tagoe who were more than generous with their expertise and precious time. In fact, this work would not have been possible without their assistance.

My special thanks also goes to my Head of Department Prof. Augustine W. K. Kyere and Dr. S.Y. Opoku (Radiotherapy Lecturer, BSc.) University of Ghana for their continue encouragement and motivation. Also my heartfelt gratitude goes to Mr. Evans Sasu (Medical Physicist, KBTH) and Mr. Linus Owusu-Agyapong (Course mate) for their immense assistance during my data collection. Not forgetting Mr. Eric KT Addison (lecturer, Dept. of Physics, KNUST) who was always there to assist and provide me with any material/equipment I needed for my work.

To all Medical Physicist, Engineers and Radiation therapist of the National Centre for Radiotherapy and Nuclear Medicine of the Korle Bu Teaching hospital, I say 'big thank' for their assistance offered throughout the entire research process.

Lastly, am grateful to the Administrator and the Director of the National Centre for Radiotherapy and Nuclear Medicine for allowing me to use their facilities for this research work.

TABLE OF CONTENTS

DECLARATION ii

ABSTRACT iii

DEDICATION iv

ACKNOWLEDGEMENTS v

TABLE OF CONTENTS vi

LIST OF TABLE x

LIST OF FIGURES xi

ABBREVIATIONS xiii

CHAPTER ONE 1

INTRODUCTION 1

1.1. Background 1

1.2. Statement of Research Problem 3

1.3. Objectives 5

1.4. Relevance and Justification 5

1.5. Scope and Limitation 6

1.6. Organization of thesis 6

CHAPTER TWO 7

LITERATURE REVIEW 7

2.1. Introduction 7

2.2. General overview of external beam radiation therapy 7

2.3. Treatment parameters in EBRT 8

2.3.1 Beam Energy 8

2.3.2 Treatment technique in EBRT 9

2.3.3 Field Size 10

2.3.4 Treatment depth 11

2.4. The Cobalt-60 teletherapy machine 12

2.4.1 Components of Cobalt-60 teletherapy machine 13

2.4.2 Treatment Couch 18

2.5. Dosimetry 22

2.5.1 Dosimetric effect of EBRT treatment couch 22

2.6. Linear attenuation coefficient 27

2.7. Transmission factor 29

2.7.1 Summary of Commonly used Transmission Factors in EBRT Dosimetry ... 30

CHAPTER THREE 32

MATERIALS AND METHODS 32

3.1. Introduction 32

3.2. Materials 32

3.2.1. Theratron Equinox 100 cobalt-60 teletherapy machine 32

3.2.2. Electrometer 34

3.2.3. Farmer-type ionization chamber 35

3.2.4. Barometer 36

3.2.5. Thermometer 37

3.2.6. Perspex slabs phantom 37

3.2.7. Locally manufactured Perspex holder 38

3.2.8. Wood species. 39

3.3. Methods 41

3.3.1. Preparation of wood samples 41

3.3.2. General Procedure and Experimental Set-up 41

3.3.3. Dosimetry measurement with the fabricated wood species 45

3.4. Data Analysis 51

CHAPTER FOUR 52

RESULTS AND DISCUSSION 52

4.1. Introduction 52

4.2. Densities of wood species 52

4.3. Determination of the linear attenuation coefficient of the wood species 53

4.3.1. Linear attenuation coefficient of the wood species at depth of 0.5cm 53

4.4. The Linear attenuation coefficient of the wood species 57

4.5. Transmission factor of the wood species 60

4.5.1. Effect of field size on transmission factor 62

4.6. Determination of the thickness of *Triplochiton scleroxylon* wood sample .. 64

CHAPTER FIVE 65

CONCLUSION AND RECOMMENDATION 65

5.1. CONCLUSION 65

5.2. RECOMMENDATION 66

5.2.1. NCRNM-KBTH 66

5.2.2. Regulatory Body 67

5.2.3. Further studies 67

REFERENCES 68

APPENDICES 75

APPENDIX A 75

APPENDIX B 86

APPENDIX C 88

APPENDIX D 90

APPENDIX E. 94

LIST OF TABLE

Table 3. 1: List of Wood species used in the Study. 40

Table 4. 1: Densities of wood species used for the study. 52

Table 4. 2: Equations obtained from figure 4.1 showing the relationship between $In\,Cor.\,Av.\,TB$ and the thickness of wood at different field size. 55

Table 4. 3: Linear attenuation coefficient of the wood species for different field size at a depth of 0.5cm. 56

Table 4. 4: Linear attenuation coefficient of the wood species for different field size at a depth of 5cm. 57

Table 4. 5: Mean linear attenuation coefficient of the wood species at the depths of 0.5cm and 5cm 59

Table 4. 6: Mean wood TFs at treatment depths of 0.5cm and 5cm using SAD setup ... 61

Table B. 1: Wawa (*Triplochiton scleroxylon*)..... 86

Table B. 2: Danta (*Nesogogordonia papaverifera*) 86

Table B. 3: Ofram (*Terminalia superba*)..... 86

Table B.4: Cedar kokote (*Entandrophragma candollei*)…….87

Table B.5: Okoro (*Albizia zygia*)…….87

Table C. 1: Wawa (*Triplochiton scleroxylon*) 88

Table D. 1: Treatment depth of 0.5cm 90

Table D. 2: Treatment depth of 5cm 92

Table E. 1: Treatment depth of 0.5cm..... 94

Table E. 2: Treatment depth of 5cm..... 94

LIST OF FIGURES

Figure 2. 1: Schematic diagram of the SSD and SAD setups 10

Figure 2. 2: Isocentric set-up technique for determining treatment depth 12

Figure 2.3: Head of a Theratron 780 treatment unit with source drawer mechanism, collimator and shielding 17

Figure 2. 4: Carbon fiber couch top 21

Figure 2. 5: EBRT couch top with wire mesh insert (a) and design of the wire mesh (b) 22

Figure 2. 6: (a) Isodose distribution used to treat the patient. (b) Grade 4 skin reaction.. 25

Figure 2. 7: (a) PA spine used in craniospinal irradiation (6 MV) and (b) Skin reaction from treatment in (a). 26

Figure 3. 1: EBRT radiation therapy (teletherapy) machine NCRNM-KBTH……33

Figure 3. 2: NE 2670 Farmer dosimeter. 34

Figure 3. 3: A 0.125 cc volume flexi cylindrical ionization chamber with the build-up cap. 35

Figure 3. 4: Precision barometer 36

Figure 3. 5: Precision thermometer 37

Figure 3. 6: Perspex slab phantom 38

Figure 3. 7: A locally manufactured Perspex holder 39

Figure 3. 8: Pictorial view of the different types of wood species used in this study 40

Figure 3. 9: A pictorial view of the general experimental set-up..... 43

Figure 3. 10: Control console or computer used in setting the beam parameters for irradiations..... 43

Figure 3. 11: Experimental Setup for Attenuation Measurement of a particular slabs of wood species for a particular field size at depth of 0.5cm. 47

Figure 3. 12: Determination of transmitted charges through the wood species at depth of 0.5cm 50

Figure 4. 1: Beam transmission as a function of the thickness of *Triplochiton scleroxylon* wood sample for the three square field sizes at a depth of 0.5cm……54

Figure 4. 2: Comparison of the TFs for the five wood species at depth of 0.5cm 63

Figure 4. 3: Comparison of the TFs for the five wood species at depth of 5cm 63

ABBREVIATIONS

RT	Radiation therapy/Radiotherapy
EBRT	External Beam Radiation Therapy
Co-60	Cobalt 60
NCRNM	National Centre of Radiotherapy and Nuclear Medicine
KBTH	Korle Bu Teaching Hospital
LINACs	Linear Accelerators
TF	Transmission Factor
FS	Field size
SAD	Source to Axis Distance
SSD	Source to Surface Distance
TPS	Treatment Planning System
3D-CRT	Three dimensional conformal therapy
dmax	Depth of maximum dose
IMRT	Intensity modulated radiation therapy
PDD	Percentage Depth Dose
Ni	Nickel
IGRT	Image guided radiation therapy
ICRU	International Commission on Radiation units and Measurement
SSDL	Secondary Standard Dosimetry Laboratory
PA	Posterior-anterior
SAR	Scatter Air Ratio
MRI	Magnetic Resonance Imaging
CT	Computer Tomography
Smic	Skin mark to isocenter

MV	Megavoltage
Gy	Gray

CHAPTER ONE

INTRODUCTION

1.1. Background

The discovery of x-rays and radioactivity 100 years ago has led to revolutionary advances in diagnosis and treatment of cancer. However, it was not until the middle of the twentieth century that megavoltage photon energies became available through the use of betatrons, cobalt-60 gamma rays and linear accelerators (linacs) [1, 2]. Radiation effectively treats cancer by targeting the tumor or cancerous cells and mutating the proliferating malignant cells so they can no longer reproduce and, therefore, die. Unfortunately, healthy cells within the patient's body can be destroyed by radiation as well [3].

In general, radiation therapy or radiotherapy is done by using brachytherapy and or EBRT (also known as teletherapy). In the case of brachytherapy, the source of radiation (usually a sealed radioactive source) is place in very close proximity to or in contact with the target volume (cancerous disease) to deliver safely high radiation dose to the target volume. In contrast to brachytherapy, EBRT directs the radiation beam at the target volume from outside the body, usually 80cm or 100cm from the target volume. In all cases, the ultimate goal of the radiation treatment is to deliver a high radiation dose to a target volume (cancerous cell) while minimizing the dose to surrounding healthy tissues as much as reasonable achievable [4, 5]. However, the latter one is the most important method or procedure in which treatment accessories such as the treatment couch becomes important.

The design of the most EBRT plan largely depends on freedom in beam incidences that can be achieved by a combination of gantry and couch rotations. With these degrees of freedom, there is a possibility for the beam to pass through the couch before entering the patient resulting in unacceptable distortion of the intended dose distribution [6, 7].

Over the years, most radiotherapy couch tops are made of materials such as carbon fiber or glass fiber [8] with some having wire mesh (designed in the form of 'tennis racket') insert at the beam incident area of the couch top and the treatment couch for EBRT procedures at the NCRNM-KBTH is of no exception of this. This is done to provide support for the patient's weight, preserve the skin sparing effect of the radiation and to eliminate attenuation of the radiation beam before traversing the patient. However, after repeated and prolonged use, the wire meshes tend to lose their elasticity causing them to yield to the weight of the patient leading to intolerable sagging culminating in setup variations. In order to circumvent this problem, the current couch tops for radiation treatment are made from solid carbon fiber without insert, fabricated in a way the couch top will have low attenuation when radiation beam passes through it [9].

Carbon fibre has become the material of choice for many radiotherapy applications, due to its strength, rigidity, low attenuation and low density [9]. Despite the advantages of carbon fiber, there are some disadvantages to the use of carbon fibre. It is expensive to use especially in the developing countries and also as conductor it can generate heat and thereby produce image artefacts on MRI scanners [10, 11]. Other composite materials have now become available that are rigid and potentially are equally radio-translucent as carbon fibre and glass fiber. As these are produced on a commercial scale and able to be fashioned in a reasonably well-equipped workshop, they could provide a cost-effective

alternative to carbon fiber and glass fiber for some radiotherapy applications. Some of these materials are non-conducting, so they could be used for MRI-compatible couch tops and accessories. One such materials is wood. However, the choice of material for EBRT couch top depends on many varied factors such as final desired transmitted radiation levels, ease of heat dissipation, resistance to radiation damage, required thickness and weight, multiple use considerations, uniformity of dose distribution within the target volume, permanence of dose transmission and availability and therefore this study aim to determine an appropriate locally fabricated wood sample with a required thickness, based on attenuation and transmission factors to be used in-place of the wire mesh couch top at the NCRNM-KBTH.

1.2. Statement of Research Problem

There are no perfect treatments for cancer, and radiation therapy is one of those imperfect treatments. Improvements are constantly being made in the field to bring it a little closer to perfection. Healthy cells can be killed along with cancerous cells causing severe damage to the patient. Delivery of correct and precise dose plays a very important role in achieving the goals of radiation treatment [12, 13, 14]. An issue in radiation therapy is the dose optimization to the target volume with minimum radiation dose to the normal surrounding tissue. However, optimization of radiation dose to a target volume during EBRT largely depends on accurate and precise patient position on the treatment couch [15]. A slight variation in the patient set-up (position) largely affect treatment outcome (prognosis). Patient treatment set-up for EBRT procedure is usually determine during target localization, where the patient is positioned on a solid couch top, usually made of

carbon fiber or glass fiber without wire mesh insert for target volume localization. Most radiotherapy centres in the developing countries also have solid carbon fiber or glass fiber without wire mesh insert, fabricated in a way the couch top will have low attenuation when the radiation beam passes through it to implement treatment set-up obtained during target volume localization for EBRT.

As a result of high cost associated with the purchasing of carbon fiber couch top, coupled with its avoidance in the treatment planning system and the skin sparing effect of radiation by wire mesh, the newly installed Theratron Equinnox-100 at the NCRNM-KBTH is equipped with treatment couch top with wire mesh insert designed in a form of "tennis racket" at the treatment area to implement the treatment set-up obtain from the target volume localization for radiation treatment. However, the wire mesh incorporated in the couch top tend to lose their elasticity after repeated and prolonged use leading to sagging, resulting in treatment set-up variation, thereby affecting dose delivery to the target volume.

To circumvent this, the current trend is to design and incorporate a wooden material at the treatment area on the couch top instead of wire mesh for EBRT clinical for clinical application. Hence, this work seeks to select a wood sample with the appropriate attenuation properties and develop quality control procedures and dosimetry protocol that make it suitable for external beam radiation treatment at the Korle Bu Radiotherapy Centre.

1.3. Objectives

The principal objective of this research is to determine dosimetric properties of a "locally fabricated" wood species for the design of couch top for external beam radiotherapy procedures.

The specific objectives of this research include:

- Determination of linear attenuation coefficient of some selected wood species and select a suitable one for clinical application.
- Determination of the effect of field size and treatment depth on the linear attenuation coefficient of the selected wood species.
- Determination of the effect of treatment field sizes on the wood couch top transmission factor using source to axial distance (SAD) treatment techniques.
- Suggestion of appropriate recommendation for the use of wood couch top for external beam radiotherapy procedures.

1.4. Relevance and Justification

This research determines linear attenuation coefficients and transmission factors, making locally fabricated wood species readily available for use in-place of wire mesh insert couch top at the NCRNM, KBTH. These values are used to determine the appropriate locally fabricated wood sample to be used in-place of wire mesh insert at the treatment area on the EBRT couch top, as well as the treatment time or monitor units calculation at a particular treatment depth and field size for radiation beam that traverses through the wooden material (in-place of wire mesh) on the couch top to the target volume. The availability of appropriate locally fabricated wood material in-place of wire mesh insert

prevents the sagging effect associated with the prolonged use of the wire mesh insert, thereby minimizing treatment uncertainties and discrepancies in dose delivery to the target volume. It also help to save money associated with the purchasing of high cost carbon fibre or glass fibre couch top for EBRT procedure. The study shall further seek to explore new applications of wood in the field of radiation therapy.

1.5. Scope and Limitation

This research is being undertaken to develop and implement a locally fabricated wooden material to be used in-place of wire mesh insert on EBRT couch top at the NCRNM and also to determine the effect of radiation field size on the transmission factor of the wooden material using SAD treatment technique to be implemented into the treatment time or monitor unit calculation for radiation beam that traverses the couch top.

1.6. Organization of thesis

This thesis is in a chronological order of five chapters. Chapter one is an introduction to the research. Chapter two reviews existing literature relevant to the research problem. Chapter three focuses on the experimental and theoretical framework for the study. The results obtained from the study are presented and discussed in chapter four and chapter five contains the conclusion of the study, recommendations and suggestions for further research.

CHAPTER TWO

LITERATURE REVIEW

2.1. Introduction

This chapter reviews relevant literature on the study. These include general overview on EBRT with respect to cobalt-60 machine and linear accelerator (linacs) coupled with the dosimetric effect of the EBRT treatment couch on the delivered dose.

2.2. General overview of external beam radiation therapy

External beam radiotherapy is a form of radiation treatment for cancer management in which the source of radiation is incorporated into a machine outside the body. In most modern EBRT, the radiation is administered in the form of x-rays or electrons, produced by a medical linacs. However, some medical facilities use gamma radiation produced by cobalt-60 teletherapy machine. The incorporating radiation source is often mounted isocentrically, allowing the beam to rotate about the patient at a fixed source to axis distance (SAD) for multiple radiation treatment fields [16].

Several specialised types of external radiation therapy may also be used to treat certain tumors. This may include; three-dimensional conformal therapy (3D-CRT), intensity modulated radiation therapy (IMRT), volumetric modulated arc therapy (VMAT), image guided radiation therapy (IGRT). Many of these techniques require well fabricated treatment couch for accurate patient position to allow the radiation beam to be delivered from several different directions. This more accurately targets the tumor and limits higher

radiation doses to surrounding normal tissues which reduces side effect associated with the delivery of the radiation beam [17].

2.3. Treatment parameters in EBRT

As the beam is incident on a patient (or a phantom), the absorbed dose in the patient varies with depth. This variation depends on many conditions: beam energy, depth, field size, treatment technique (SSD or SAD), and beam collimation system. Thus the calculation of dose in the patient involves considerations in regard to these parameters as they affect depth dose distribution [18, 19].

2.3.1 Beam Energy

Typical radiation beam energies usually used in EBRT are 6 MV, 8 MV, 10 MV or 15 MV for high energy photon beams (such as linacs), cobalt-60 units for low energy photon beams (that is an average of 1.25 MV), and 6 MeV, 10 MeV and 15 MeV for electron beams; with each energy producing different central axis depth dose distribution. The central axis depth dose distribution depends on the beam energy; and as a result, the depth of a given isodose curve increases with beam quality. The absorbed dose in the medium outside the primary beam is greater for low-energy beams than for those of higher energy. Physical penumbra depends on beam quality. Thus, one disadvantage of the orthovoltage beams is the increased scattered dose to tissue outside the treatment region. For megavoltage beams, on the other hand, the scatter outside the field is minimized as a result of predominantly forward scattering [19].

2.3.2 Treatment technique in EBRT

Basically there are two main types of treatment technique in EBRT. Source to surface/skin distance (SSD) and Source to axis/axial distance (SAD).

In a clinical or dosimetry setting, either SSD or SAD setup can be used; however, the most widely used value of SSD or SAD for clinical practice is about 100 cm [18]. These treatment techniques tend to affect the amount of dose deposited in a medium. Clinical application of SSD technique is usually used to treat skin lesion usually lymph nodes lesion. Dosimetric measurement involving this technique takes place at the depth of maximum dose (d_{max}) usually 0.5 cm beneath the skin surface for cobalt-60 teletherapy machines. Radiation treatment calculations involving SSD technique use percentage depth dose (PDD) curves and are easier to measure in a phantom. With more modern treatments using multiple fields, the use of a constant SSD technique leads to frequent patients repositioning between treatments [19]. However, unlike SSD technique, SAD techniques are mostly used to treat deep-seated tumour. Modern EBRT treatment techniques have an isocenter that the teletherapy machine rotates around. Rather than repositioning the patient for every beam, the constant SAD technique (isocentric technique) uses the same distance from the beam source to the isocenter. This leads to problems in dose calculation, percentage depth dose calculations are based on a certain source to surface/skin distance. This may be overcome by the use of tissue-air, tissue-phantom or tissue-maximum ratios, which adjust dose based on the depth within the patient and not on the source surface distance [19].

The field size for SSD setup is usually defined at the surface of the phantom, whilst for the SAD setup, the field size is defined at the detector position (isocenter). Figure 2.1 shows a schematic diagram of both the SSD and SAD setup.

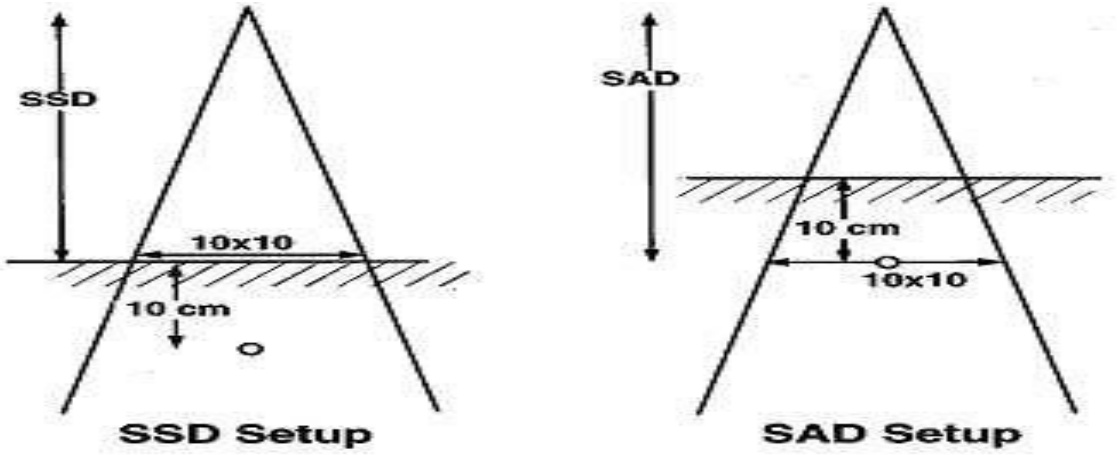


Figure 2. 1: Schematic diagram of the SSD and SAD setups

2.3.3 Field Size

Field size is one of the most important parameters in treatment planning and hence, dosimetric procedures. Adequate dosimetric coverage of the tumor requires a determination of appropriate field size. This determination must always be made dosimetrically rather than geometrically. In other words, a certain isodose curve enclosing the treatment volume should be the guide in choosing a field size rather than the geometric dimensions of the field [18, 19].

Field size is defined at a point which is normally placed at the isocenter of the treatment machine. Radiation fields are divided into two types: geometric and dosimetric (physical) field sizes. According to the ICRU, the geometric field size is define as ‘the projection of

the distal end of the machine collimator into a plane perpendicular to the central axis of the radiation beam as seen from the front centre of the source'. The dosimetric field size (physical field size) is defined by the intercept of a given isodose surface (usually 50%) with a plane perpendicular to the central axis of the radiation beam at a defined distance from the skin. Zero area fields are a hypothetical radiation fields in which the dose at depth 'z' in a phantom is entirely due to the primary photons, since the volume that can scatter radiation is zero [19].

In effect, as the field size increases, peak scatter factor increases from unity linearly and saturates at very large fields. Also, the beam quality at which the maximum back scatter occurs shifts toward harder radiation with an increase field size.

2.3.4 Treatment depth

This is the distance beneath the skin where the target volume can be located. Clinically, it can be found by the use of diagnostic procedures such as CT-scan, MRI-scan or Ultrasound of the anatomical site to be treated. For a typical EBRT treatment set-up involving isocentric technique (Figure: 2.2), the treatment depth is determine by the difference between the SAD of the teletherapy machine and the SSD of the particular radiation field [19]. However, SSD EBRT treatment technique has a constant treatment depth of 0.5cm (d_{max}) for dose fall (cobalt-60 teletherapy machine). Other radiation treatment procedures such as RT of spine and lymph node of breast cancer have constant treatment depth based on research. Treatment depth plays a major role in EBRT dosimetry. It is usually involved in the radiation treatment time calculation for EBRT procedures [19].

The larger the field size, the deeper the depth of the peak and the larger the scatter function. The larger the depth in phantom, the smaller is the relative primary component and the larger the relative scatter component.

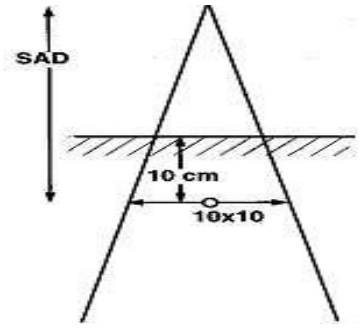


Figure 2. 2: Isocentric set-up technique for determining treatment depth

2.4. The Cobalt-60 teletherapy machine

A major advantage of cobalt units is the basic simplicity of their design and construction that generally makes them inherently reliable. Compared to modern linear accelerators, cobalt-60 teletherapy units offer poorer geometrical precision in treatment because of a larger penumbra and greater mechanical inaccuracy. Cobalt can no longer provide the basis for contemporary sophisticated radiation therapy. This is because cobalt beams are less penetrating than those from linear accelerators and they also lack the flexibility in the control of the radiation output offered by linear accelerators. However, commercially available cobalt units may be quite adequate for many palliative treatments, and there are even some applications where cobalt sources have been used in specially designed equipment to give a performance that could be argued to be superior to that obtainable from a conventional linac. Some of these applications include stereotactic radiosurgery

with the Elekta Gamma Knife [20, 21] and total body irradiation with custom-designed extended source skin distance (SSD) units [22]. Cobalt-60 teletherapy is the most appropriate choice for radiotherapy in countries where facilities for the linacs are lacking [23]. Many of the major techniques and advances in the physics of external beam radiation therapy were developed on cobalt units. These include arc therapy, conformal therapy, transmission dosimetry, the development and measurement of tissue air ratios and the subsequent derivation of scatter air ratios (SARs), and differential SARs and the associated algorithms for treatment planning based on the separation of primary and secondary radiation [24]. Poffenbarger and Podgorask [25] have investigated the possibility of using an iso-centric unit for stereotactic radiosurgery, and Warrington and Adams [26] have shown that conformal therapy, and even IMRT, could be adequately delivered with a cobalt-60 unit except for the most deep-seated tumors.

2.4.1 Components of Cobalt-60 teletherapy machine

A major advantage of cobalt units is the basic simplicity of their design and construction that generally makes them inherently reliable. Nevertheless, care must be taken to ensure that they are robustly built and carefully maintained to minimize the potential hazards from the high activity source and the associated heavy shielding. A complete cobalt-60 teletherapy machine consists of various components and the following sub-sections look at the major components of the cobalt-60 machine.

2.4.1.1 Radiation source

Application of cobalt-60 radionuclide as a teletherapy radiation source was first put to clinical use in 1951 [27, 28]. Although megavoltage x-ray beam had been available for some years prior to this date, they were not in widespread use, whereas cobalt-60 radionuclide became the mainstay radiation source for EBRT procedures worldwide. The cobalt source usually consists of a series of either millimetre-size cylindrical pellets or thin, metallic discs sealed within a double capsule of stainless steel and manufactured to meet certain standards regarding protection from impact, corrosion, and heat [29]. A double welded steel is use to prevent any leakage of the radioactive material during transport. A typical teletherapy ^{60}Co source is a cylindrical shape of diameter 2cm, height 5cm, and is positioned in the Cobalt Unit with the circular end facing the patient. About 25% of the primary photons are lost in a typical source due to self-attenuation. The fact that the radiation source is not a point source also complicates the beam geometry and gives rise to what is known as the geometric penumbra and the transmission penumbra. These penumbras create a region of dose variation at the field edges. Important characteristics of ^{60}Co radionuclide as a teletherapy radiation source are its high gamma ray energy couple with its high specific activities and relatively long half-life [30].

The radioactive cobalt-60 (chemical symbol Co, atomic number of 27 and atomic weight 58.933 amu) with half-life of 5.27 years is derived from the bombardment of cobalt-59 with neutron in a nuclear reactor. The radiation source (^{60}Co) is usually housed in the gantry head, which is part of the teletherapy machine. It consist of a steel filled with lead for shielding purposes as well as a pneumatically driven source drawer for moving the source between shielded position and treatment position to produce clinical usefulness of

the gamma ray beam. The radiation source is usually replaced within one half-life after it is installed, however, financial considerations result in longer source usage. The ^{60}Co source decays to ^{60}Ni by β - decay. Two separate γ-ray decays occur at 1.17 and 1.33 MeV from ^{60}Ni. The emitted gamma ray constitute the therapy beam whereas the electron beam is absorbed in the source capsule [30].

2.4.1.2 The Head

The head of a cobalt unit has three basic functions: to shield the source, to expose the source as required, and to collimate the beam to the correct size. Shielding is achieved by surrounding the source and exposure mechanism with lead and, in many designs, with alloys of a higher density metal such as tungsten in order to reduce the volume. In some earlier designs, depleted uranium alloy (with a high percentage of U238, density approximately 19.0×10^{3} kgm^{-3}) was used, but this has been discontinued because of the problems with stability of the alloy as some of it became powdery and also because of the difficulties associated with eventual disposal [30].

The source exposure mechanism is usually one of two types; either the source is moved between a safe and exposed position (as shown in Figure: 2.3) or where the source remains stationary, and a moving shutter opens or closes the beam. The latter solution, implemented on earlier machines is now obsolete. In the former solution, the source movement is either a translation or a rotation and is the same mechanism explored by Theratron® Equinox™-100 teletherapy machine at the NCRNM-KBTH. The machine has source-to-skin distance of 100 cm, which is an important parameter of the machine. It is achieved by the compact design of source head and collimator. Various beam collimator

designs exist to give variable rectangular fields with sides ranging in length, typically, from 4 cm to 30 cm or even up to 40 cm on iso-centric units with a source axis distance (SAD) of 100 cm. Each of the four collimator leaves is usually focused on the edge of the source proximal to it so as to avoid cut-off of the primary beam and minimize penumbra. Distances from the source to the far edge of the collimators are typically between 40 cm and 50 cm for machines designed for 80 cm SSD, but this distance may be increased by penumbra trimmers that are particularly desirable when the machine is to be used for 100 cm SSD treatment. With careful design of the collimation system and a 15 mm diameter source, a penumbra of no more than 10 mm (distance between the 20% and 80% decrement lines) may be achieved at 5 cm depth for field sizes with an area of less than 20×20 cm^2 [30]. The source head also house some important features such as Optical Distance Indicator to display the distance between the source and the skin.

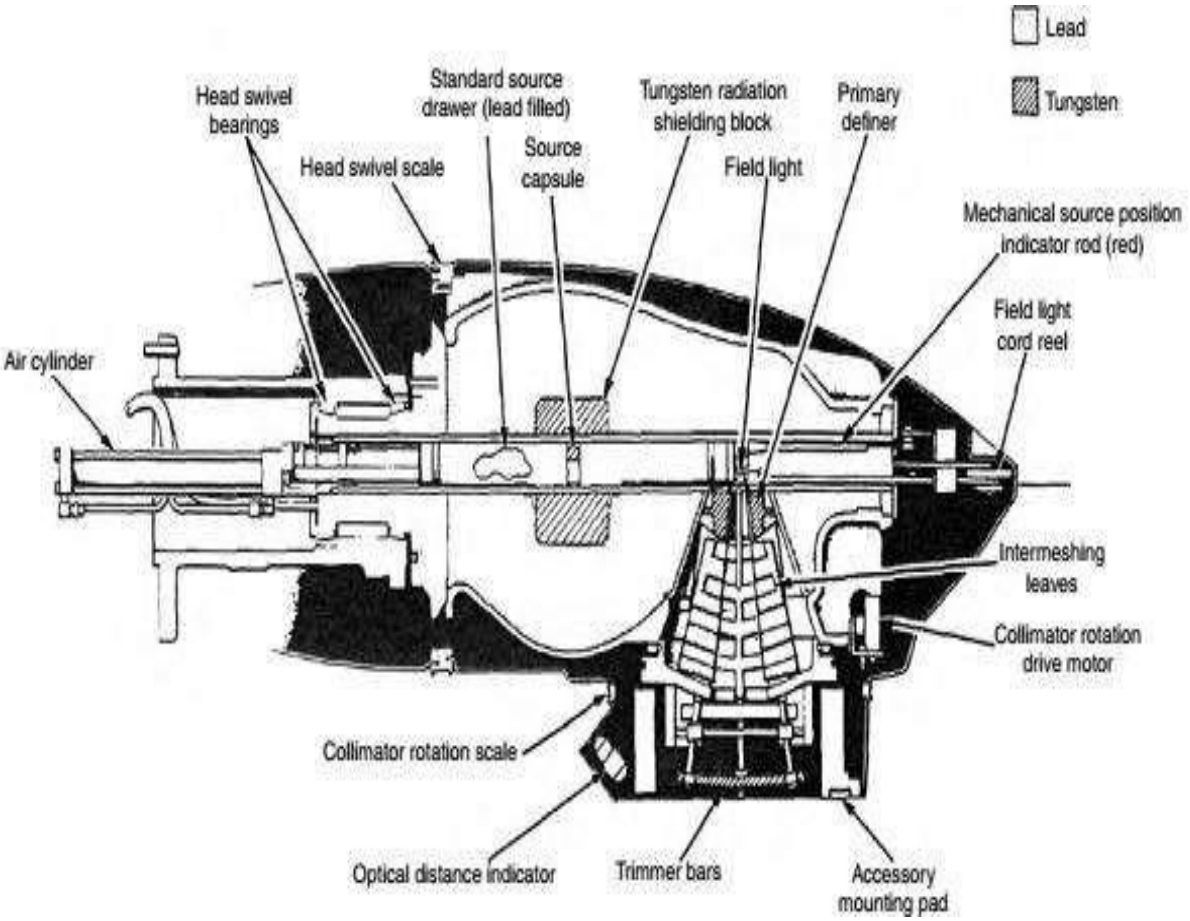


Figure 2.3: Head of a Theratron 780 treatment unit with source drawer mechanism, collimator and shielding.

2.4.1.3 Gantry

The gantry is the part of the unit that holds the source head and counter weights. It is mounted on the base housing. In order to obtain a reasonable compromise between output, depth dose, and clearance around the patient, modern cobalt units are manufactured in a standard iso-centric configuration with a source axis distance of 80 cm being the most common [31]. Units with an SAD of 100 cm are also practical if high activity sources can be afforded and offer the advantages of greater depth dose, larger field sizes, greater

clearance around the patient, and geometrical compatibility with linacs. In order to increase their versatility, iso-centric units have often been made with the ability to swivel the head about a horizontal axis through the source by ±180°.

This swivel motion keeps the beam axis in a vertical plane, and when used with an appropriate gantry angle, may be useful for extended SSD treatments or for treating immobile patients in a bed or chair. Some non iso-centric cobalt units have been manufactured with the head held by a yoke on a vertical stand, and these are particularly useful for giving single field palliative treatments. Where an iso-centric unit has the swivel facility, great care must be taken to ensure that its position is accurately reset before the equipment is used, since the slightest angulation of the head swivel is likely to create a large deviation of the beam axis from the mechanical iso-centre. Some iso-centric units use slip rings for the supply of all power and control signals to the gantry and this allows continuous gantry rotation. Coupled with the guaranteed constant output from the source as the unit rotates, such a versatile and simple rotation mechanism provides an ideal unit for arc or full rotation therapy when this technique is required [31].

2.4.2 Treatment Couch

The Co-60 unit has a sophisticated patient support system on which the patient has to sit or lie down during treatment. It consists of a turntable mounted eccentrically with the isocenter to support another system of tables providing required motions for positioning the tumour site at the isocenter. All the motions are motorised and the couch is under fully computerised control. The indexed patient positioning system enables quick, accurate and reproducible patient positioning [32]. Several unique features of the couch top provide the

top with mobility that allows accurate patients positioning. However, unlike the couch top on the simulator, patients may be positioned at either end of the treatment couch depending on the treatment plan [32].

2.4.2.1 Basic construction of EBRT couch top

Due to intensive use of treatment couch in clinics for radiation treatment procedures, finding an optimum material for the designing of the couch top becomes important. However, in an effort to improve EBRT treatment, specialized treatment couch, usually carbon fibre couch top without wire mesh insert (Figure: 2.4) is used to position cancer patients for radiation treatment to circumvent dose discrepancies associated with the use of couch top with wire mesh insert. Carbon fiber couches for EBRT procedures are usually made of flat panels, each consisting of two carbon fiber plies separated by a layer of filler substance. The use of the filler adds extra strength to the material by introducing a gap between the two sheets of carbon fiber materials [33].

Carbon fiber is a material with high tensile strength and rigidity; extremely light with low specific density and relative radio-translucence. Studies have shown low attenuation of the radiation therapy beam by carbon fiber treatment couches. Also studies comparing the properties of three commercially available carbon fiber inserts with those of conventional inserts over a range of clinically relevant energies have shown that carbon fiber inserts attenuates high-energy photon beam by less than 1% [34]. However, due to the assumption that, carbon fiber is an air-equivalent material and therefore its avoidance in the treatment planning system coupled with the high cost associated with the purchasing of carbon fiber couch top for EBRT procedure, many radiotherapy centres have adopted different

treatment couches with removable wire mesh insert (Figure 2.5) at the beam incident area of the couch top which have almost no limitation in choosing beam angles in treatment planning and also increases the skin sparing effect of radiation beam.

Given the necessity for the radiation treatment couch to be rigid enough to support large patients without sagging, the construction material of the treatment couch top has two important constraints: it must be strong and durable enough to meet manufacturer's sag tolerances and must be radio-translucent enough to minimize the effect of attenuation of the therapy beam when radiation beam intersect the couch top [34, 35]. Hence, the loss of elasticity of the wire mesh insert on EBRT couch tops as a result of prolonged use requires the exploration of new, possibly more rigid, radio-translucent and locally fabricated material such as wood in-place of the wire mesh insert at the treatment area of the couch top.

A number of authors have recommended the use of treatment couch top in the treatment planning system either because of its highly attenuating components and/or because of concerns about increase in skin dose. Some studies have shown that the treatment couch is not negligible during treatment planning process whereas the dose delivering is performed with treatment couch [36]. As a result of the potential influences of the treatment couch on treatment planning system coupled with radiation transmission, a lot of studies have been carried out involving treatment couch [37, 38, 39, 40]. For instance, Gillis *et al.* [37] evaluated the Sinmed Mastercouch and revealed 1.5% attenuation for 5 cm × 5 cm field size for both 6 MV and 18 MV photons. Spezi and Ferri [38] evaluated a Siemens IGRT tabletop and found that for a 10 cm × 10 cm field size, a 6 MV photon was attenuated by 2.1%. Njeh *et al.* [39] reported that for normal incidence, a beam

attenuation of 3.4% to 4.9% for 6 MV photon and 0% to 0.7% for 18 MV photons for the BrainLAB ICT was observed. Independently, McCormack *et al.* [40] also documented 2.2% 6 MV photon beam attenuation for Sinmed Posisert couch for direct incidence of $10\,\text{cm} \times 5\,\text{cm}$ field size, while Muthuswamy [41], reported on a general analytical equation that could be used to determine whether a beam would intersect components of the treatment couch. Accounting for support structures of the treatment couch significantly reduced differences between planned and delivered dose. The difference between planned and the measured dose could be reduced to less than 2% if the couch was included in the TPS [42]. In the case of Varian IGRT couch, even though the exact position of the couch was found to be unimportant because of its high uniformity, inclusion of the couch in the TPS avoided clinically dosimetric discrepancies [43].



Figure 2. 4: Carbon fiber couch top

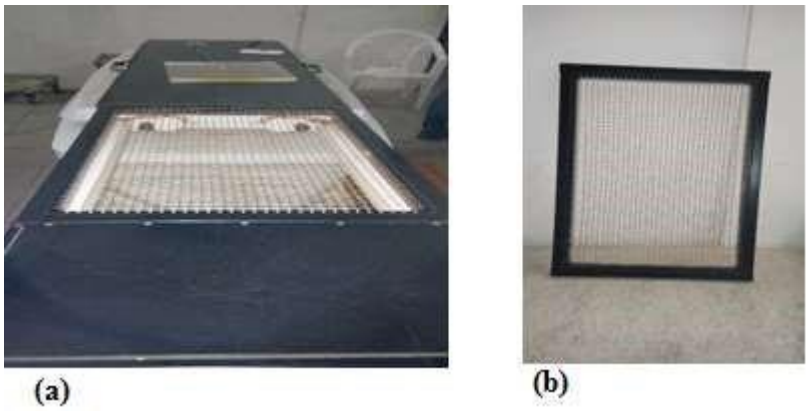


Figure 2. 5: EBRT couch top with wire mesh insert (a) and design of the wire mesh (b)

2.5. Dosimetry

Radiation dosimetry is the process whereby a signal is recorded through interactions of incident radiation with matter causing a measureable change in its properties. This can be a change in the measured charges (ionization chambers), measured light output (TLD) or visible polymeric chemical reaction (radiochromic film). The process is caused by atomic and nuclear interactions occurring within the atom [30].

Dosimetry is the measurement of the absorbed dose delivered by ionizing radiation, the term is better known as a scientific sub-specialty in the fields of health physics and medical physics, where it is the calculation and assessment of the radiation dose received by the human system [30, 44].

2.5.1 Dosimetric effect of EBRT treatment couch

Devices remote from the patient act primarily as attenuators and scatterers whilst devices close to the patient act like bolus, increasing the skin dose and shifting the depth dose

curve toward the patient surface [45]. With the introduction of volumetric modulated arc therapy (VMAT), a significant portion of the target dose is delivered through the couch top (and rails when present), creating a renewed interest in evaluating dose perturbations such as attenuation, increased skin dose, and target coverage effects.

The dosimetric impact from devices such as EBRT couch top external to the patient is a complex combination of increased skin dose, reduced tumor dose, and altered dose distribution; the magnitude being a function of beam energy, relative geometry of the beam, the fraction of dose delivered through the couch top, and its physical composition [46].

2.5.1.1 Effect on skin dose

From the early days of radiotherapy, skin was used as a "dosimeter" (erythema dose) and there is a significant knowledge base for skin dose-response. Archambeau *et al.* [47] provides an excellent discussion of the pathophysiology, anatomy, and dose response of the skin, describing clinically observed skin and hair changes as a function of total dose and fraction size. Skin doses over about 25 Gy at 2 Gy per fraction produce clinically relevant skin reactions and greater than 45 Gy may produce dry desquamation [47]. The radiosensitivity of the skin is often enhanced by concomitant chemotherapy or near sites of surgical intervention while larger doses per fraction, commonly used in stereotactic radiotherapy, exacerbate the skin reaction for the same total dose [48].

There are many well-known clinical situations where skin dose can be excessive (e.g., skin folds, electron or Orthovoltage beams, bolus). However, the impact of couch tops is

often not well recognized. Kry *et al.* [49] recently presented a review of all factors affecting skin dose in radiotherapy. Numerous publications show a significant increase in surface dose when beams first transit carbon fiber couch tops at either normal or oblique incidence [50] and show these to be larger than for the mylar-covered tennis racket couch top. However, the sagging effect, associated with the prolonged used of the mylar-covered tennis racket couch top increases dose discrepancies within the target volume.

The clinical importance of skin dose is often overlooked when treating with megavoltage photon beams, where the clinical goal is to eradicate deep seated tumors. However, clinically relevant skin toxicity due to the passage of beams through the couch top has been reported [51]. Hoppe *et al*. [48] described one case of grade 4 skin toxicity in patients undergoing large dose per fraction stereotactic body radiotherapy using three posterior 6 MV beams passing through the treatment couch top and immobilization device (Figure:2.6). The original plan failed to include the dosimetric effect of these devices which resulted in the skin dose of about 50% while subsequent replanning simulating the inclusion of these devices revealed a 90% skin dose [48]. This skin reaction was attributed to a combination of all posterior beams, a target volume close to the skin surface, and the intervening external devices (treatment couch top and immobilization devices).

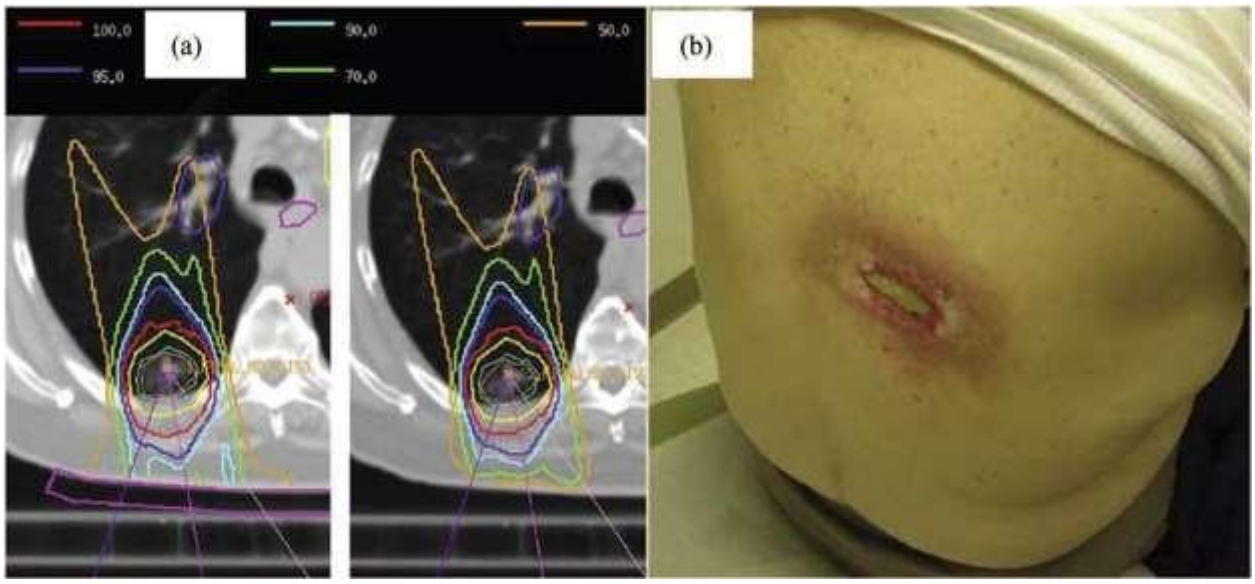


Figure 2. 6: (a) Isodose distribution used to treat the patient. (b) Grade 4 skin reaction

Another clinical example, a medulloblastoma patient treated supine on an IGRT couch top, is shown in (Figure. 2.7). The prescribed dose was 23.4 Gy in 1.8 Gy fractions to the craniospinal axis. The spinal dose was prescribed to 5 cm depth using a PA field. Post treatment revealed a grade 2–3 skin reaction on the patient's back, which was more prominent at the superior aspect of the spine field. The maximum superficial dose from this treatment was ≥ 29 Gy (2.2 Gy/fraction) and much of the increased skin dose was due to treatment through the carbon fiber couch top.

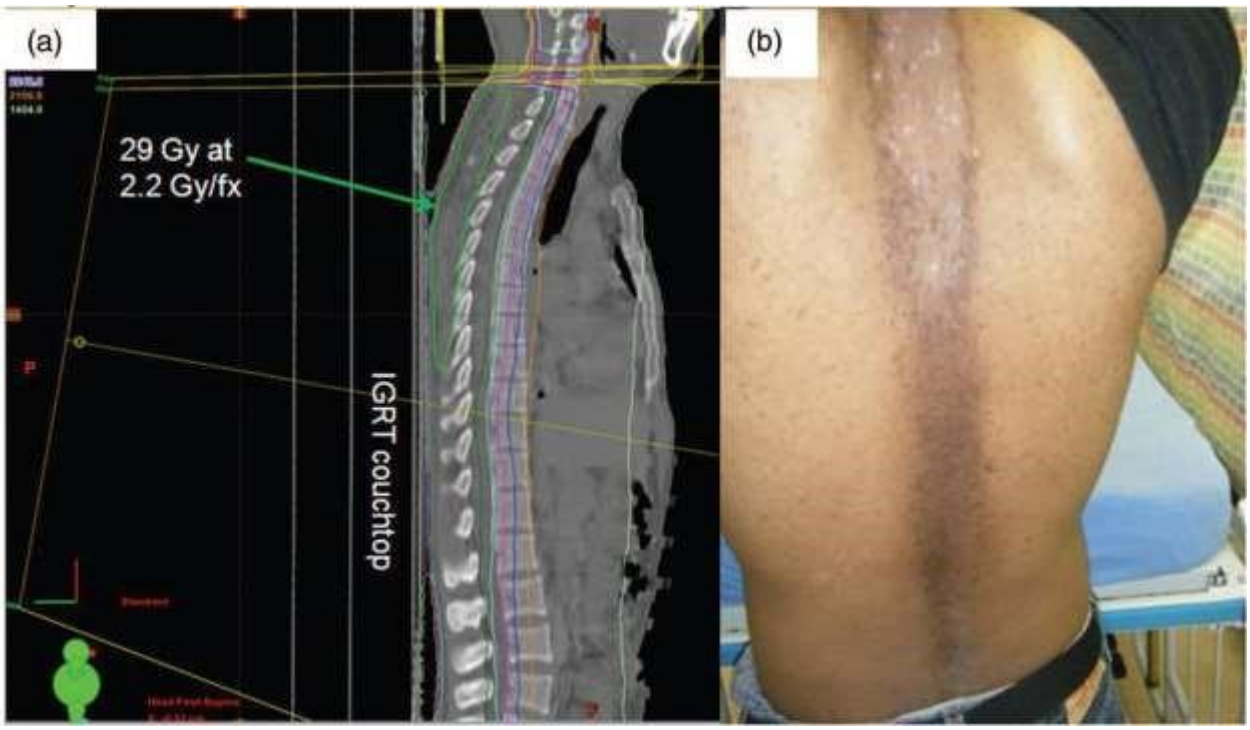


Figure 2. 7: (a) PA spine used in craniospinal irradiation (6 MV) and (b) Skin reaction from treatment in (a).

2.5.1.2 Effect on beam attenuation

In addition to increasing skin dose, patient supporting system (treatment couch) also attenuate the photon beam. Prior to carbon fiber couch tops, the most attenuating portion of most couches was the high Z center spine or side rails. Krithivas and Rao presented early work on the issue by examining the attenuation of a 4 MV beam by the center-spine of a Clinac 4/100 couch where 60◦ posterior arcs resulted in dose reductions of 8%–12% [52]. Sharma and Johnson expanded on this work, including attenuation due to couch side rails [53]. For modern carbon fiber couch tops, attenuation of up to 15% can be seen for certain parts of the couch top. As expected, attenuation increases with decreasing photon energy, increasing angle of incidence to the couch, and to a lesser extent, increasing field

size. Most researchers give attenuation data for just one field size, usually 10 × 10 cm^2. However, Myint *et al.* showed about 1% difference in attenuation for 6 MV for 5 × 5 cm^2 and 10 × 10 cm^2 when the magnitude of attenuation was 7% (through a strut). Several reports showed that couch attenuation can increase 4-fold as the beam angle ranges from 0◦ to 70◦ [54].

2.6. Linear attenuation coefficient

Studies on interaction of gamma radiation have been the subject of interest for the last several decades. Study of gamma-ray interaction has made profound impact in the fields of atomic physics, radiation physics, material science, environmental science, biology, health physics, agricultural, cancer therapy and forensic science etc. As a γ-ray passes through a medium, an interaction occurs between the photons and matter resulting in energy transfer to the medium [55]. The interaction can result in a large energy transfer or even complete absorption of the photon (beam attenuation). However, a photon can be scattered rather than absorbed and retain most of the initial energy while only changing direction [55].

Attenuation coefficient is an important parameter for study of interaction of radiation with matter that gives us the fraction of energy scattered or absorbed. When a photon passes through an attenuator material, the probability that an interaction will occur depends on its energy, the composition and thickness of the attenuator [56]. The thicker the attenuator material, the more likely an interaction will occur. The change in X-ray or gamma beam

intensity at some distance in an attenuator (or an absorber) for narrow mono-energetic beam is governed by the Beer Lambert equation given below [30];

$$I=I_O e^{-\mu x} \qquad (2.1)$$

Where

I: the intensity of the photon beam transmitted through an attenuator

X: the thickness of the attenuator

I_o: the initial intensity of the photon beam.

The quantity μ is the linear attenuation coefficient of the attenuator material. The minus sign indicates the beam intensity decreases with increasing attenuator thickness. The linear attenuation coefficient represents the 'absorptivity of the attenuating material. The quantity μ is found to increase with linearly with attenuator density ρ. This value can be used to calculate values such as the intensity of the energy transmitted through an attenuating material, intensity of the incident beam or the thickness of the material. It may also be used to identify the material if the previously mentioned values are already known [30].

Taking natural log to both sides of equation (1) gives

$$In\ I = In\ I_o - \mu x \qquad (2.2)$$

The linear attenuation coefficient describes the fraction of intensity of X-rays or gamma rays that is absorbed or scattered per unit thickness of an attenuating material in the path of the radiation beam.

2.7. Transmission factor

Radiation dose transmission is a concern when dealing with materials in the path of radiation beam during EBRT treatment. Some materials may be attenuating more radiation beam than others, however, these materials are usually accounted for their transmission factor in the treatment time or monitor unit calculation for EBRT treatment. When X-rays or γ-rays traverse matter, some are absorbed, some pass through without interaction, and some scatter as low energy photons in directions that are different from those in the primary beam. Transmission factors generally increases with decrease values of μ. Values of μ generally increase as the atomic number, *Z*, of the absorbing material increases because photoelectric interactions are increased in high-*Z* materials, especially for low-energy photons. The most effective gamma transmissions are materials which have a low density and low *Z*.

Based on Peebles and Plesset [57], a study has been conducted on the feasibility of accurate numerical determination of the transmission of gamma-rays through large thickness of materials. They further explained that approach to the gamma-ray transmission problem was based on the notion that one needs to consider only those transmitted gamma-rays which have suffered relatively few scattering even for thickness of approximately twenty mean free paths.

According to Beer's law, transmitted intensity I_t is describe as transmission factor as T_f

$$T_f = \frac{I_t}{I_o} = e^{-ux}$$

Where T_f is the transmission factor through a thickness x (cm) of a material in the path of the beam and I_o , beam incident on the material [30].

2.7.1 Summary of Commonly used Transmission Factors in EBRT Dosimetry

Transmission Factor	Definition of terms	Dependent treatment parameters
Wedge factor	This depicts the amount of the radiation transmitted through a physical wedge placed in the beam to shape the beam delivery. A wedge is made of a dense material, usually lead or steel which attenuates the radiation beam progressively across the field. The thinner side of the wedge attenuates less of the beam than the thicker side, resulting in an alteration of the beam isodose patterns [30]	Energy of the beam, treatment depth and field size
Tray factor	The ratio of the radiation transmitted through a block tray with respect to the amount of radiation that incident on the tray. Most block tray are made of plastic derivatives. When the beam of radiation hits the tray, some amount of the radiation beam is attenuated by the tray. The radiation beam not attenuated by the tray then passes through the tray and continue to the target volume [30].	Energy of the beam, and field size
Output factor	It is the ratio of the dose in phantom at a given reference depth for a given field size to the dose at the same point and depth for the reference field size. It is commonly known as total scatter factor and can be broken up into two components, collimator and flattening filter scatter and scatter arising from interactions in the phantom [30].	Energy of the beam, treatment depth and field size

Collimator scatter factor	This is the ratio off output in air for a given field size to that of the reference field size. The field size are define by the collimator setting on the entire build up cap with the measurement taken in air with ion chamber. Build-up cap used for such study provides dose scatter equilibrium [30]	Energy of the beam, treatment depth and field size
Phantom scatter factor	It is the ratio of dose for a given field size to that for the reference field size measured at the same depth. This account for the changes in scatter originating in phantom or patient as the field size changes [30].	Energy of the beam, treatment depth and field size

CHAPTER THREE

MATERIALS AND METHODS

3.1. Introduction

This chapter outlines the materials and methods used for the study. The design and fabrication of wooden species and the procedures used to conduct the research work are also included. The experimental study and/or data collection was carried out at the NCRNM- KBTH.

3.2. Materials

The materials used in this study includes; five (5) different wood species; Theratron Equinox 100 cobalt-60 teletherapy machine; An electrometer, Farmer type ionization chamber, Perspex slab phantom, Perspex holder, Digital thermometer and Barometer. Detailed description of these materials are presented below.

3.2.1. Theratron Equinox 100 cobalt-60 teletherapy machine

The Theratron 100 cobalt-60 teletherapy machine was used for the quality control and dosimetric measurements on the fabricated wooden species. This machine is a fully computerized isocentric teletherapy machine employed in the treatment of malignant (cancer) and benign tumours at the NCRNM. The machine is incorporated with a unique features such as availability of smaller and larger field sizes of (0.2cm x 0.2cm) and (42cm x 42cm) respectively, rotatable gantry and collimator, availability of symmetric and

asymmetric collimator jaws coupled with physical and motorize wedges, unit head panel, hand control, control console with display monitor and treatment couch with wire mesh insert at the treatment area as shown in Figure 2.8.

The source of radiation employed by this teletherapy machine is Co-60 radioisotope with half-life of 5.26 years. The Co-60 radioisotope is sealed in a double layer stainless steel capsule such that the diameter of the whole source assembly is 2.0 cm and 3.0 cm long. During treatment, the Co-60 atoms spontaneously decay to Ni-60 with emission of beta particle and two gamma radiations of energies 1.17 MV and 1.33 MV. The beta particle is usually absorb in the capsule whilst the gamma radiation constitute the therapy beam. The energy of the therapy beam is taken as the mean of the two stipulated energies of the gamma radiations above as 1.25 MV.

The radiation source is being operated by a two ways air cylinders using compressed air during and after RT. The two ways cylindrical compressed air is use to drive the source from a fully shielded position (beam off position) to a fully exposed position (beam on position) during EBRT procedure.

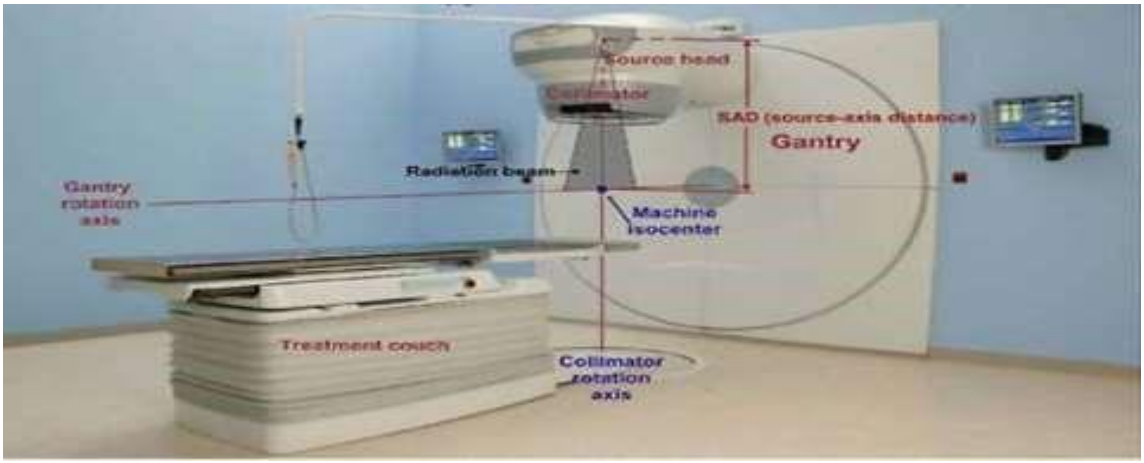


Figure 3. 1: EBRT radiation therapy (teletherapy) machine NCRNM-KBTH

3.2.2. Electrometer

There are numerous kinds of electrometers for dosimetry procedures in radiation therapy, diagnostic radiology and nuclear medicine, however the electrometer used for this study at the NCRNM, KBTH was NE 2670 farmer dosimeter (Figure 3.2) from Thermo electron corporation model with serial number 431. It is suitable for secondary standard calibration and offers excellent stability and easy operation. It is able to repeat readings within ±0.05% and display them in five (5) digit floating point. The electrometer displays the measured values of dose in gray (Gy) or Sievert (Sv) or Rontgen (R) and dose rate in gray per minute (Gy/min) or Sievert per hour (Sv/hr),or Rontgen per minute (R/min) whiles measured values of electrical charges and currents are display in coulomb (C) and ampere (A) respectively.



Figure 3. 2: NE 2670 Farmer dosimeter.

3.2.3. Farmer-type ionization chamber

A 0.125 cc volume flexi cylindrical ionization chamber type; 2532 with serial number 0851 was used for the study. It is the most popular cylindrical ionization chamber designed by Farmer, hence Farmer-type ionization chamber and originally manufactured by PTW, Freiburg, Germany, but now available from several vendors, for dosimetry procedures in radiotherapy, especially in EBRT. Its chamber sensitive volume resembles a thimble, and hence the Farmer type chamber is also known as a thimble chamber. The chamber has a good uniform response to radiation over a wide range of energies, hence preferred means of measuring high levels of gamma radiation. The chamber (Figure 3.3) was calibrated with a known beam quality source and a bias voltage of 400 V at the IAEA Secondary Standard Dosimetry Laboratory (SSDL) under the following standard conditions; Temperature (T) of 293K, Pressure (P) of 101.325kPa and Relative Humidity (RH) of 50%.



Figure 3. 3: A 0.125 cc volume flexi cylindrical ionization chamber with the build-up cap.

3.2.4. Barometer

This is a scientific instrument for measuring atmospheric pressure. The precision barometer (Figure 3.4) with serial number L991133 was used to record the atmospheric pressure at the treatment room during measurements under different environmental conditions. The atmospheric pressure value recorded was used to account for the dosimetric measurement obtained by the ionization chamber, calibrated under standard atmospheric pressure of 101.32kpa specified by the Secondary Standard Dosimetry Laboratory (SSDL).



Figure 3. 4: Precision barometer

3.2.5. Thermometer

This is a scientific instrument for measuring temperature. The precision thermometer (Figure 3.5) with serial number L991133 was used to record the temperature at the treatment room during measurements under different environmental conditions. The temperature value recorded was used to account for the dosimetric measurement obtained by the ionization chamber, calibrated under standard temperature of 293k specified by the Secondary Standard Dosimetry Laboratory (SSDL).



Figure 3. 5: Precision thermometer

3.2.6. Perspex slabs phantom

There are numerous phantoms (devices that mimics human tissues) for dosimetric study. However, the Perspex slabs phantom (figure: 3.6) was used in this study. It is a form of Plexiglas phantom, chemically composed of $(C_5O_2H_6)n$. It has mass density (g/cm^3) between (1.16 – 1.20)g/cm^3 with number of electrons per gram and effective atomic number of 3.24×10^{23} and 6.84 respectively. It was specially manufactured by PTW for

dosimetric measurement. It has a size of 30cm x 30cm with different thicknesses ranging from 0.5cm to 1cm. However, among these thickness of Perspex slabs phantom is the 2 cm thick slab with a hole provided on one of its sides by the manufacturer to hold the 0.125 cc farmer type ionization chamber.

The use of this phantom help to achieve the different treatment depths associated with target volume localization for dosimetric measurement by increasing the number of Perspex slabs to stimulate the treatment depth.



Figure 3. 6: Perspex slab phantom

3.2.7. Locally manufactured Perspex holder

A locally manufactured Perspex holder was used to support the wood species in the path of the radiation beam for the dosimetric study. The Perspex holder (figure: 3.7) with the following dimensions: length=20cm, width=20cm and height=16cm was made up of

Perspex slab of thickness 0.5cm. It has a volume capacity of 6400cm^3 with both ends (top and bottom) open to minimize the effect of attenuation by the Perspex slabs.



Figure 3. 7: A locally manufactured Perspex holder

3.2.8. Wood species.

Wood from all conifers is classified as soft wood, while the wood from all other trees which have broad leaves is termed hardwood. Woods have a variety of uses; in the field of radiation science, they can be used to shield radiation from nuclear sources. However, in order to fully understand wood properties and its behaviour when subjected to physical, chemical and biological processes, there is need for future research on wood. The list of wood species used for this study are presented in the Table 3.1 and Figure 3.8 shows the pictorial view of these selected wood species.

Table 3. 1: List of Wood species used in the Study.

S.NO	Scientific Name	Trade/Common Name	Type
1	*Triplochiton scleroxylon*	Wawa	Softwood
2	*Nesogogordonia papaverifera*	Danta	Hardwood
3	*Terminalia superba*	Ofram	Hardwood
4	*Entandrophragma candollei*	Cedar kokote	Hardwood
5	*Albizia zygia*	Okoro	Softwood

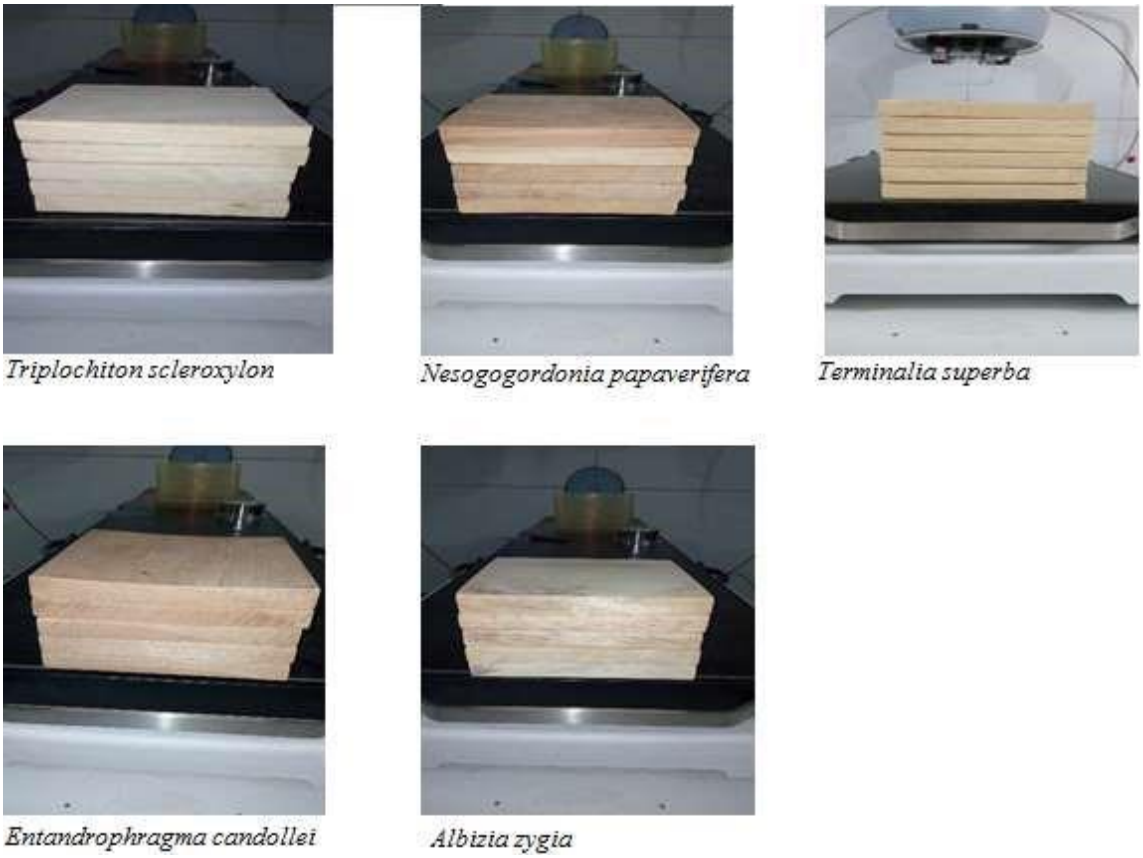


Figure 3. 8: Pictorial view of the different types of wood species used in this study

3.3. Methods

This involves the determination of linear attenuation coefficient and transmission factor of the five (5) selected wood species (Figure: 3.8) and their dependencies on field size using SAD techniques for measurement.

3.3.1. Preparation of wood samples

Five (5) different types of wood species (Figure: 3.8) were collected and designed from well-equipped workshop (Accra). The selection of these wood species were based on their availability and ability to withstand stress associated with EBRT couch top.

Each wood sample was nicely designed and cut into six (6) square slabs (Figure 3.8) of equal dimensions: 20.0 cm by 20.0 cm with 2.5cm thickness for irradiation. The wood samples were dried up at a room temperature of 28°C for a period of 120 days. During this time they were weighed continuously and their weights monitored until the rate of change in weight became less than 0.1 % per day. They were then considered stable to changes in moisture content with time and ready to be used for the dosimetric procedure.

3.3.2. General Procedure and Experimental Set-up

As part of data collection for the study, Perspex slab phantoms and the fabricated wood species selected for the study (after preparation) were left in the air conditioned radiation treatment room for one week. This was to allow both materials to assume the room temperature [58].

Prior to the measurements, (for determination of linear attenuation coefficient and transmission factor of the wood species), eleven (11) Perspex slabs with each having dimensions of: length=30cm, width=30cm and thickness=1cm were nicely arranged perpendicularly along the central axis of the beam on the cobalt-60 couch top. Among the Perspex slabs for the study was a special slab with the same dimensions as above but with 2cm thickness, demarcated smic on one of it surfaces and a 'hole' provided on one of its side by the manufacture to hold the ion chamber during dosimetry procedures. The 'hole' is usually 0.5cm from the surface with demarcated smic and 1.5cm from the opposite surface. The 2cm thickness Perspex slab was gently and uniformly placed on top of the eleven Perspex slabs arranged on the couch top such that the distance from the couch top and distance from the surface of the phantom to the 'hole' were 12.5cm and 0.5cm respectively. The Perspex slabs were used to simulate the human body, which provided an electronic equilibrium for the measurements. An ionization chamber (Figure 3.3) connected to an electrometer (Figure 3.2) at the control console room (Figure: 3.10) via a cable, was then placed in a Perspex slab phantom (positioned on the treatment couch top) via 2cm thickness Perspex slab chamber 'hole' provided on one of its side by the manufacture. The ion chamber was then adjusted such that its tip (sensitive part) was at the iso-centre of the phantom which coincided with the central axis of the radiation beam (iso-centre of the radiation beam) and the intersection of the transverse and longitudinal lasers on the surface of the phantom. This was to enable the chamber detect most interacting charges. The general experimental set-up was as shown in the Figure: 3.9.



Figure 3. 9: A pictorial view of the general experimental set-up



Figure 3. 10: Control console or computer used in setting the beam parameters for irradiations.

The ionization chamber was configured to measure charges with a bias voltage of + 400 V at 60sec interval on the electrometer connected to it. The ionization chamber was then pre-irradiated for 300 seconds (5 mins) in a Perspex slab phantom placed on the treatment couch to liberate stray charges in the chamber, in order to avoid residual charges in the chamber being measured [58]. Constancy test was also performed to ensure consistent readings from the chamber using cobalt-60 teletherapy machine and the Perspex slab phantom (Figure: 3.6).

The outputs of the cobalt-60 teletherapy machine for the determination of linear attenuation coefficient and the transmission factors of the wood species were measured for a field sizes of 5cm x 5cm, 10cm x 10cm and 15cm x 15cm using SAD techniques at treatment depths of 0.5cm and 5cm for each wood sample. For the determination of transmitted beam through different thickness of wood for a particular wood sample at a treatment depth of 0.5cm and 5cm for a field size of 5 x 5cm^2, 10 x 10cm^2 and 15 x 15cm^2, a locally manufactured Perspex holder was inserted at the collimator jaw (as shown in Figure 3.9) to hold the wood for the measurement. Throughout the experiment, the gantry angle and collimator angle were set at 0^0.

For each measurement involving a particular field size or thickness of wood sample, readings were repeated three (3) times using integration time of 60secs per reading on the electrometer connected to the chamber with a constant radiation treatment time of 300secs (5 minutes) set on the radiation monitor at the control console. The mean or average reading for a particular field size or thickness of the wood sample was calculated and used for the study. The procedure was repeated for the different field size and thickness of wood selected for the study for the various wood species. In all measurement, the ambient

pressure and temperature at the treatment room before and after irradiation were measured with precision barometer (figure: 3.4) and thermometer (Figure: 3.5) respectively to estimate for the mean temperature and pressure correction factor to account for the effect of temperature and pressure on the average output (electrometer readings) measured at a particular point (field size or thickness of wood) using the formula:

$$K[T,P]=\left[\frac{273.15+T_C}{293.15}\right]\times\frac{101.3}{p}=\frac{273.15+(\quad)}{293.15}\times\frac{101.3}{(\quad)}=$$

For temperature and pressure correction factor determination and

$$Cor.ERD = K[T,P] \times Average\ ERD$$

Where T = Average temperature for each measurement

P = Average pressure during measurement

Cor.ERD = Corrected electrometer readings

3.3.3. Dosimetry measurement with the fabricated wood species

3.3.3.1. SAD setup for wood species Attenuation Coefficient Measurements

This technique (or setup) takes into consideration the distance from the source to the detector or point of measurement within the phantom as well as the treatment depth. For

the purpose of this study, a constant treatment depth of 0.5cm and 5cm were used. The treatment depth describes the distance from the surface of the phantom to the point of the detector (ion chamber) along the central axis of the beam.

With referenced to the general procedure and experimental setup (Figure 3.9) described above, the treatment couch was then adjusted such that the SSD at the isocenter of the Perspex slab which also coincided with the tip of the ion chamber (sensitive part) read 99.5cm, coinciding with a depth of 0.5cm in the phantom. With this setup obtained on the treatment couch, a locally manufactured Perspex holder (Figure 3.7) was then fixed at the collimator jaw of the gantry head such that the distance from the inferior end of the Perspex holder to the surface of the phantom was 25cm (Figure 3.9). The Perspex holder was used to support the slabs of the wood species in the path of the radiation beam. For a particular wood species, field sizes of 5 x 5cm^2, 10x10cm^2 and 15x15m^2 at SSD of 99.5cm (depth of 0.5cm) were used to irradiate the ionization chamber with the various thickness of the wood (selected for the study) in the path of the radiation beam for an integration time of 60 seconds (1.0 minute) on the electrometer and radiation treatment time of 300 seconds (5 minute). Transmitted charges (transmitted beam) through the wooden material for a particular thickness of the wood were collected and measured using the ion chamber and the electrometer respectively. Three successive readings were taken for a particular thickness of the wood species at a particular field size and the average values determined. The initial and final temperatures and pressures were recorded using a thermometer and barometer respectively and the calculated temperature and pressure correction factor at different thickness of wood were used to account for the effect of temperature and pressure on the average values obtained at the various thickness.

This same procedure was then repeated for the rest of the wood species and their average transmitted electrometer readings were corrected for the effect of temperature and pressure. The experimental setup is as shown in Figure 3.11 for a particular wood sample at a particular field size at depth of 0.5cm.



Figure 3. 11: Experimental Setup for Attenuation Measurement of a particular slabs of wood species for a particular field size at depth of 0.5cm.

The whole procedure was then repeated for a treatment depth of 5cm. However, to obtain this depth from the general experimental setup (Figure 3.9) a 4.5cm Perspex slab, made up of four (4) Perspex slabs with each having a thickness of 1cm and a special 0.5cm Perspex slab with equal dimensions in terms of length and width as the one used in the general procedure were uniformly and nicely arranged on top of the 2cm Perspex slab holding the ion chamber to simulate the treatment depth from the surface of the phantom to the ion chamber as 5cm or SSD of 95cm for the measurement.

3.3.3.2. Background on Attenuation.

The attenuation of gamma radiation is due to the effect of all the energy exchange mechanism such as Photoelectric effect, Pair production and Compton Effect. The

transmitted intensity depends on the density; thickness of the absorbing layer and the cross-sectional properties of the material [57]. When gamma radiation of intensity I_o is incident on a material of thickness x, the attenuation of the gamma radiation by the material is given by the relationship.

$$I=I_O e^{-\mu x} \qquad (3.1)$$

Where I_o is the intensity of the incident radiation, x is the thickness of the material, I is the intensity after passage.

Taking natural log to both sides of equation (1) gives

$$In\ I = In\ I_o - \mu x \qquad (3.2)$$

Hence, a graph of *In I* against x (thickness of the wood) gives a gradient of the graph which is equal to the negative of the linear attenuation coefficient of the particular wood species.

For a particular wood species, the linear attenuation coefficient was determined for the various field sizes at a particular depths selected for the study using equation (3.2). The effect of field sizes and depths on the linear attenuation coefficient were also determined

3.3.3.3. SAD setup for wood species TF measurements.

With referenced to the general procedure and experimental setup (Figure 3.9) described above, the treatment couch was then adjusted such that the SSD at the isocenter of the Perspex slab which also coincided with the tip of the ion chamber (sensitive part) read

99.5cm, coinciding with a depth of 0.5cm in the phantom. With this setup obtained on the treatment couch, an open field at SSD of 99.5cm, field sizes of 5 x 5cm^2, 10x 10cm^2 and 15 x 15cm^2 were used to irradiate the ionization chamber for 60 seconds (1.0 minute) integration on the electrometer using radiation treatment time of 300 seconds (5 minute). Charges were collected and measured using the ion chamber and the electrometer respectively. Three successive readings were taken for each field size and the average values determined. The initial and final temperatures and pressures were recorded using a thermometer and barometer respectively and the calculated temperature and pressure correction factor at different field size were used to account for the effect of temperature and pressure on the average values obtained at the various field size. Note that this open field values for the field size were used for all types of wood species selected for the study.

This same procedure was then repeated with each of the wood species in the path of the radiation beam (figure 3.12). The transmitted charges through the wood were collected and the average value corrected for the effect of temperature and pressure.

The whole procedure was then repeated for a treatment depth of 5cm by increasing the number of the Perspex slabs beyond the ion chamber by 4.5cm thickness to simulate a depth of 5cm from the surface of the phantom to the detector (ion chamber) along the central axis of the beam.

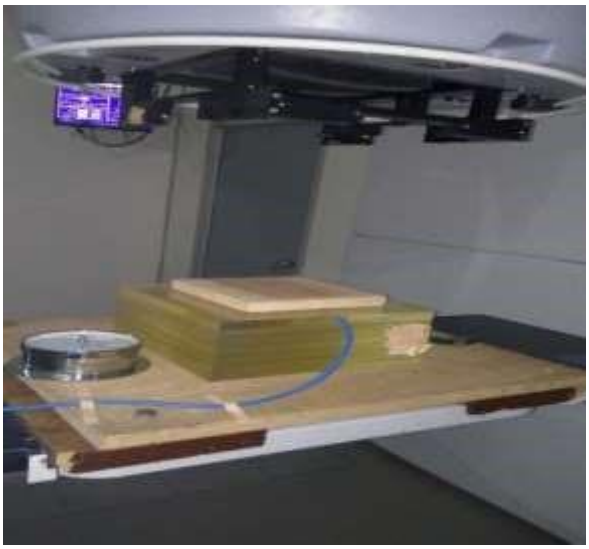


Figure 3. 12: Determination of transmitted charges through the wood species at depth of 0.5cm

Transmission factors were then calculated for the different wood species at different field sizes under the two treatment depths. This was done by dividing the corrected electrometer readings with and without the wood species in the path of the radiation beam for each field size. The equation for TFs is given as:

$$TF = \frac{Radiation\ dose\ with\ a\ beam\ modifier}{Radiation\ dose\ without\ a\ beam\ modifier} \quad (3.3)$$

Hence, to calculate for the wood transmission factor, it is given by the equation:

$$Wood\ TF = \frac{Radiation\ dose\ with\ wood\ in\ the\ path\ of\ the\ beam}{Radiation\ dose\ without\ the\ wood\ in\ the\ path\ of\ the\ beam} \quad (3.4)$$

For a particular wood species, the transmission factors at different field sizes were compared to determine the effect of field size on the transmission factors. Also for a

particular field size, the transmission factors for the various wood species selected for the study were compared to choose a wood species suitable to replace the wire mesh insert.

3.4. Data Analysis

Due to the large number of data obtained, the Excel programming software was used to analyse the results obtained from the measurement. The version used was that of Microsoft word 2013 plus; and this was used to calculate the average temperature, pressure and electrometer readings throughout the work. The software program was also used to calculate for the corrected readings for temperature and pressure and the transmission factor of the wood species using equations 3.4. Also the Excel program was used to plot various graphs in order to analyse the data obtained from the measurements.

CHAPTER FOUR

RESULTS AND DISCUSSION

4.1. Introduction

This chapter presents and discusses the results obtained from the study. Transmission Factors for all the wood species selected for the study coupled with their corresponding linear attenuation coefficient were determined at different field sizes (5 x5 cm^2, 10 x 10 cm^2, 15 x 15 cm^2) using SAD technique. This was used to determine a required wood sample, considered dosimetrically suitable to be used in place of wire mesh insert. The effect of field size on the transmission factor and the linear attenuation coefficient of the wood species were also determined and analysed.

4.2. Densities of wood species

The densities of the wood samples were determined by measuring their masses and dimensions as given in Table 4.1

Table 4. 1: Densities of wood species used for the study.

Wood samples	**Length/ cm**	**Breadth/ Cm**	**Thickness/ cm**	**Volume/cm^3**	**Mass/g**	**Density g/cm^3**
Wawa	20	20	2.5	1000	420	0.42
Danta	20	20	2.5	1000	1100	1.1
Ofram	20	20	2.5	1000	780	0.78
Cedar kokote	20	20	2.5	1000	720	0.72
Okoro	20	20	2.5	1000	600	0.60

4.3. Determination of the linear attenuation coefficient of the wood species

The linear attenuation coefficient of the wood species were determined under two treatment depths: 0.5cm and 5cm using SAD technique for field sizes of 5 x 5 cm^2, 10 x10cm^2 and 15 x 15cm^2 stipulated for the study. For a particular wood sample, a graph of natural logarithm of the corrected average transmitted beam /charges $I_n\,(Cor.Av.TB)$ as presented at Appendix B and C was plotted against the thickness of the wood type. The equation obtained from the graph for each radiation field was then compared to Beer Lambert equation modified as equation 3.2 to determine the linear attenuation coefficient and intensity of the incident radiation for the wood sample. Average linear attenuation coefficient and intensity of the incident radiation across the radiation fields were therefore calculated for each wood sample at different depth.

4.3.1. Linear attenuation coefficient of the wood species at depth of 0.5cm

Linear attenuation coefficient of the various wood species selected for the study were determined at a depth of 0.5cm using the data presented at Appendix B. A graph of $I_n\,(Cor.Av.TB)$ was plotted against the thickness of the wood for a particular wood type.

4.3.1.1. Linear attenuation coefficient of Wawa (*Triplochiton scleroxylon)* Wood

From the data presented at Appendix B (Table B.1), a graph of $I_n\,(Cor.Av.TB)$ on the vertical axis was plotted as a function of the thickness of wood on the horizontal axis for the three stipulated field sizes used for the study.

Figure 4.1 below is a plot obtained from the graph of the $I_n\,(Cor.Av.TB)$ against the thickness of wood (Wawa (*Triplochiton Scleroxylon*) for three square field sizes at depth of 0.5cm.

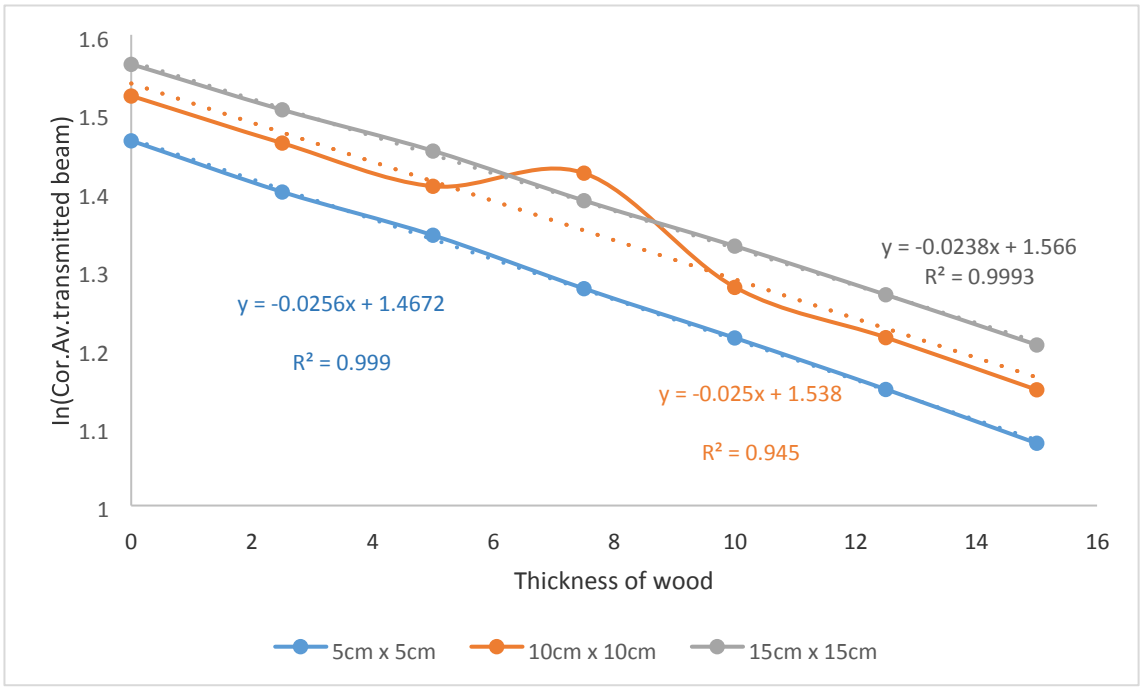


Figure 4. 1: Beam transmission as a function of the thickness of *Triplochiton scleroxylon* wood sample for the three square field sizes at a depth of 0.5cm

From Figure 4.1, blue line is the graph of $I_n\,(Cor.Av.TB)$ against thickness of *Triplochiton scleroxylon* wood sample for the 5x 5cm^2 field size,

Brown line and grey line are the corresponding graphs for the 10cm x 10cm and 15cm x 15cm field sizes respectively.

The corresponding $I_n\,(Cor.Av.TB)$ as a function of the thickness of wood (*Triplochiton scleroxylon)* equation obtained from the Figure 4.1 for the determination of linear

attenuation coefficient and intensity of the incident radiation of *Triplochiton scleroxylon* at different field sizes were presented in the table 4.2 below:

Table 4. 2: Equations obtained from figure 4.1 showing the relationship between $I_n\,(Cor.Av.TB)$ and the thickness of wood at different field size.

Equation	Field sizes	I_0/nC
$I_n\,(Cor.Av.TB) = -0.0256t + 1.4672$	5cm x 5cm	1.4672
$I_n\,(Cor.Av.TB) = -0.025t + 1.538$	10cm x 10cm	1.5380
$I_n\,(Cor.Av.TB) = -0.0238t + 1.566$	15cm x 15cm	1.5660

From Table 4.2, comparing equation (3.2) to the equations obtained at different field sizes from the graph of $I_n\,(Cor.Av.TB)$ /nC against thickness of wood (t), it implies the magnitude of the gradient obtained from the graph correspond to the linear attenuation coefficient of the wood at a particular field size.

Therefore for a field side of 5cm x 5cm with an equation of $I_n\,(Cor.Av.TB) = -0.0256t + 1.4672$.

The gradient 0.0256cm^{-1} is the linear attenuation coefficient (μ) of the wood (*Triplochiton scleroxylon*) for stipulated field side of 5cm x 5cm at a depth of 0.5cm.

The corresponding linear attenuation coefficient of the same wood species (*Triplochiton scleroxylon*) for the field sizes of 10cm x 10cm and 15cm x 15cm were determined using the same method as 0.025cm^{-1} and 0.0238cm^{-1} respectively. The average μ and I_0 were calculated as 0.0248cm^{-1} and 1.5237nC respectively.

The same method, as described above for the determination of linear attenuation coefficient of Wawa (*Triplochiton scleroxylon*) was used to determine the linear attenuation coefficient of the rest of the wood species at the stipulated depths using their corresponding data at Appendix B and C for a depth of 0.5cm and 5cm respectively to plot a graphs of $I_n\ (Cor.Av.TB)$ against the thickness of the wood type.

The linear attenuation coefficient of the wood species, together with the average intensity of the incident beam determined at a depth of 0.5cm and 5cm were therefore presented in the table below as table 4.3 and 4.4 respectively as a function of one side of a square field.

Table 4. 3: Linear attenuation coefficient of the wood species for different field size at a depth of 0.5cm.

	One side of a square field/cm				
wood species	5cm	10cm	15cm	Average μ /cm^{-1}	Average I_0/nC
Wawa	0.0256	0.025	0.0238	0.0248±0.0009	1.524±0.051
Danta	0.0584	0.0564	0.0540	0.0563±0.0022	1.521±0.051
Ofram	0.0323	0.0312	0.0300	0.0312±0.0012	1.519±0.049
Cedar kokote	0.0414	0.0417	0.0399	0.0410±0.0010	1.509±0.049
Okoro	0.0369	0.0352	0.0337	0.0353±0.0016	1.515±0.050

Table 4. 4: Linear attenuation coefficient of the wood species for different field size at a depth of 5cm.

	One side of a square field/cm				
wood species	5cm	10cm	15cm	Average μ /cm^{-1}	Average I_0/nC
Wawa	0.0271	0.0248	0.0239	0.0253±0.0017	1.379±0.084
Danta	0.0613	0.0568	0.0545	0.0575±0.0035	1.375±0.081
Ofram	0.0326	0.0311	0.0300	0.0312±0.0013	1.393±0.096
Cedar kokote	0.0388	0.0423	0.0358	0.0390±0.0033	1.381±0.081
Okoro	0.0403	0.0366	0.0352	0.0374±0.0026	1.380±0.089

4.4. The Linear attenuation coefficient of the wood species

The linear attenuation coefficient denoted by the symbol ($\mathcal{U}$) describes the fraction of a beam of x-rays or gamma rays that is absorbed or scattered per unit thickness of the absorber.

From the measurement carried out, the linear attenuation coefficient for each of the wood species used was determined for three different field sizes of 5cm x 5cm, 10cm x 10cm and 15cm x 15cm at two stipulated depths 0.5cm and 5cm using SAD radiation treatment technique. These linear attenuation coefficient are presented at table 4.3 and table 4.4 for treatment depth of 0.5cm and 5cm respectively. From the tables (both table 4.3 and 4.4), linear attenuation coefficient for each of the wood sample generally decreased as the field

size increased. This effect was more pronounced at a depth of 0.5cm, which implies at this depth, with the wood species in the path of the radiation beam more of the delivered radiation dose get to this point when the field size increase. This effect was as a result of increased scatter which constituent the dose delivered at a point (depth) in a medium. Scatter increases as field size increases, as there are more volume or field occupy by the radiation which result in an increased electrons production as a result of interaction of radiation with the medium. These increased number of electrons, therefore contribute to the dose at that point. However, there was disparity in this trend for *Entandrophragma candollei* wood sample. The linear attenuation coefficient for this type of wood species increased slightly from a field size of 5cm x 5cm to 10cm x 10cm and then decreased at the field size of 15cm x 15cm. This effect was observed for both treatment depth of 0.5cm and 5cm. The effect was as result of non-uniform composition of the wood. Such wood species was therefore not suitable to be used in-place of wire mesh as there could be a differential attenuation of the radiation beam for radiation treatment field that traverse a wood couch resulting in dose inhomogeneity in the target volume. This effect would be difficult to be accounted for in the TPS system for dose optimization in the target volume.

In order to obtain a single linear attenuation coefficient for each of the wood species that can be compared and select a suitable wood type to be used in-place of the wire mesh insert couch top, the mean linear attenuation coefficient for each of the wood species with their deviation was calculated at depth of 0.5cm and 5cm. The values obtained is shown in the table 4.5 below.

Table 4. 5: Mean linear attenuation coefficient of the wood species at the depths of 0.5cm and 5cm

	Treatment depths	
Wood species	0.5cm	5cm
Triplochiton scleroxylon	0.0248 ±0.0009	0.0253±0.0017
Nesogogordonia papaverifera	0.0563±0.0022	0.0575±0.0035
Terminalia superba	0.0312±0.0012	0.0312±0.0013
Entandrophragma candollei	0.0410±0.0010	0.0390±0.0033
Albizia zygia	0.0353±0.0016	0.0374±0.0026

From (table 4.5.), linear attenuation coefficient of the wood species increases from the depth of 0.5cm to the depth of 5cm. However, *Triplochiton scleroxylon* recorded the lowest attenuation coefficients among the various wood samples considered for gamma-rays of average energy 1.25MV. This was followed by *Terminalia superba* and *Albizia zygia* (Table 4.5). *Nesogogordonia papaverifera* has the highest linear attenuation coefficients.

Besides *Triplochiton scleroxylon* which consistently had the lowest linear attenuation coefficient for the two treatment depths, the other wood species such as *Entandrophragma candollei* had fluctuating linear attenuation coefficient. This could be due to variations in wood structure and constituents. The attenuation coefficient of any material is directly proportional to its density [30], however, this study shows some inconsistencies in the attenuation coefficient-density relationship for wood samples considered for the study.

For example, *Albizia zygia* with density of 0.60g/cm^3 had mean linear attenuation coefficient of (0.0353±0.0016) cm^{-1} and (0.0374±0.0026) cm^{-1} at a depth of 0.5cm and 5cm respectively while *Terminalia superba* with density 0.78g/cm had linear attenuation coefficient of (0.0312±0.0012) cm^{-1} and (0.0312±0.0013) for the same treatment depths of 0.5cm and 5cm respectively. Thus, it was seen that even though *Albizia zygia* had lower density than *Terminalia superba* the latter had a lower linear attenuation. This could be so because linear attenuation does not depend on density alone but also on other factors such as the chemical, physical and mechanical properties of the wood. In addition the densities of the wood determined in this study were the apparent densities (which are highly water content dependent) and not the true density. The nature of the wood has a substantial influence on the linear attenuation. The structure and the inherent constituents of the wood influence its strength and radiation beam attenuations capacity. This also explains why due to the wood structure a less dense wood such as *Albizia zygia* could have higher linear attenuation than a denser wood like *Terminalia superba*.

4.5. Transmission factor of the wood species

Transmission factor for each of the wood sample was among the basic requirements for selecting a suitable material to be used to replace the wire mesh insert couch top.

From the measurements carried out, the TF for each of the wood species selected for the study was obtained for various field sizes at two different treatment depths of 0.5cm and 5cm using SAD setup. These TFs are shown Appendix E1 and E2 for the treatment depth of 0.5cm and 5cm respectively. In order to obtain a single wood transmission factor that

can be compared and incorporated into dose calculation during treatment planning, the mean wood TF for each of the wood sample with their deviation was calculated for the depths of 0.5cm and 5cm using SAD setup. This is shown in Table 4.6.

Table 4. 6: Mean wood TFs at treatment depths of 0.5cm and 5cm using SAD setup

	Treatment depth/cm	
Wood species	0.5cm	5cm
Triplochiton scleroxylon	0.979±0.003	0.947±0.008
Nesogogordonia papaverifera	0.948±0.011	0.893±0.019
Terminalia superba	0.981±0.003	0.952±0.009
Entandrophragma candollei	0.972±0.006	0.938±0.011
Albizia zygia	0.965±0.007	0.921±0.014

From Tables 4.6, it can be observed that, treatment depth has effect on transmission factors of the various wood species selected for the study. This effect was seen as a decrease in transmission factor as treatment depth increased from 0.5cm to 5cm. The effect was attributed to the fact that, at an increased depth, there is more attenuation of the radiation beam by the underlying tissue or phantom than at a shallow depth, hence radiation treatment with this wood species in the path of radiation beam requires treatment time calculation accounting for the transmission factor of these wood species to dispute dose discrepancies associated with their use at a particular depth. The effect of treatment depth on transmission factor of these wood species was also in accordance with a study conducted by Opoku *et al.* [58]

Terminalia superba recorded the highest transmission factor among the various wood samples considered. This was followed by *Triplochiton scleroxylon* and *Entandrophragma candollei* (Table 4.6). *Albizia zygia* and *Nesogogordonia papaverifera* had the lowest transmission factor in that order. However, the transmission factor of *Terminalia superba* was not in accordance with its linear attenuation coefficient, as it shown an increased in linear attenuation coefficient. This effect could be attributed to the structural constituent of the wood and therefore such wood species cannot be used to replace the wire mesh, as there could be a differential attenuation of the radiation beam, thereby affecting dose delivered to the target volume. The transmission factor for the *Triplochiton scleroxylon* was the second highest and this was in accordance with its low linear attenuation coefficient compared to the rest of the wood samples and therefore such wood sample can be used to replace the wire mesh to minimize dose discrepancies associated with the sagging effect of the wire mesh.

4.5.1. Effect of field size on transmission factor

Appendix E1 and Appendix E2 show that at a depth of 0.5cm and 5cm respectively, measured TFs increased as field sizes increased from 5cm x 5cm to 15cm x 15cm. This is mainly as a result of the increase in electron scattering from the collimators, air and the wood species in the path of the beam. This is in agreement with other results in literature [19, 30], all of which reported an increase in TFs with increasing field size. (Figures 4.2 and 4.3)

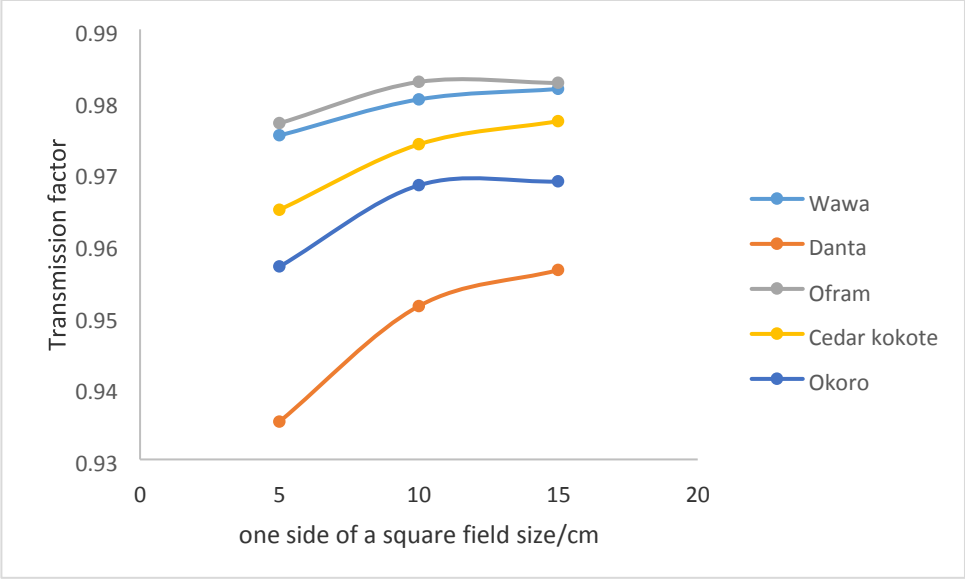


Figure 4. 2: Comparison of the TFs for the five wood species at depth of 0.5cm

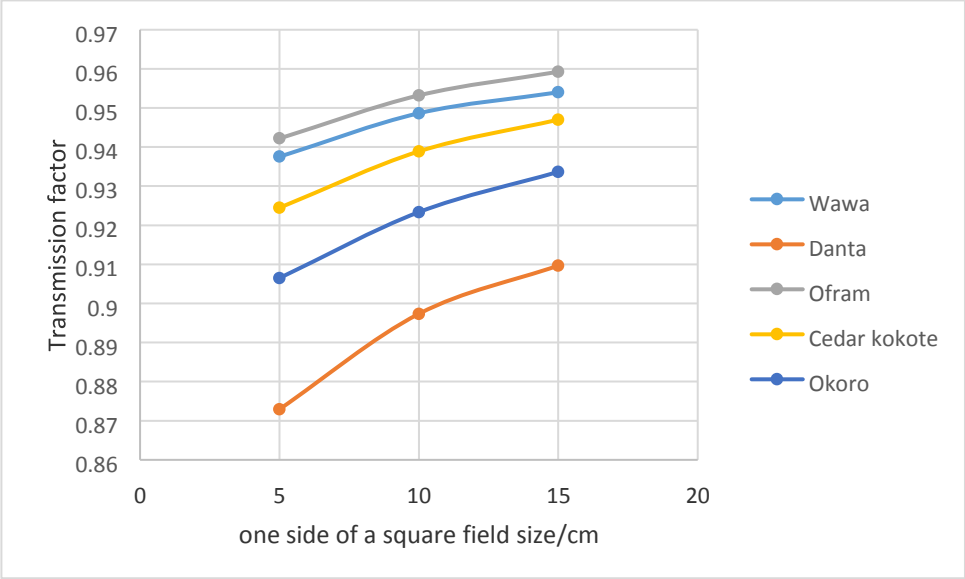


Figure 4. 3: Comparison of the TFs for the five wood species at depth of 5cm

4.6. Determination of the thickness of *Triplochiton scleroxylon* wood sample

For the purpose of dose transmission, a material for the design of couch top should allow at least 95% of radiation dose through it.

Hence, $\frac{I}{I_O} X\ 100 = 95\% = 100e^{-\mu x}$ 4.1

Therefore

$0.95 = e^{-\mu x}$ (Applying natural logarithm to both side)

$$\ln 0.95 = -\mu x \quad 4.2$$

Given average μ of Wawa (*Triplochiton scleroxylon)* as: 0.0248cm^{-1}

Putting 0.0248cm^{-1} into equation 4.2, the value of x (thickness) of wood in centimetre is given as approximately 2cm.

Therefore the required wood thickness to be used to replace the wire mesh insert is approximately 2cm.

CHAPTER FIVE

CONCLUSION AND RECOMMENDATION

5.1. CONCLUSION

The linear attenuation coefficient and the transmission factor of the wood species selected for the study were found to depend on the field size as well as the treatment depth and therefore, a single transmission factor of beam modifying devices used in treatment planning system for time calculation or monitor units should be considered at different treatment depths and field sizes associated with target volume localization to account for effect of radiation dose on these radiation treatment accessories. It was observed that in terms of radiation beam transmission, the *Triplochiton scleroxylon* wood sample with lowest linear attenuation coefficient (Table 4.5) and second highest transmission factor (Table 4.6) was more suitable than other tested wood samples for replacing wire mesh insert at the treatment area of the EBRT couch top. The percentage deviation of its linear attenuation coefficient at a depth of 0.5cm and 5cm was 3.63% and 6.72% respectively whilst that of transmission factor was 0.31% and 0.84% at the same depths respectively. *Terminalia superba* had highest transmission factor (Table 4.6) with mean deviation of 0.31% and 0.94% at a depth of 0.5cm and 5cm respectively. The highest transmission factor of *Terminalia superba,* however was not in agreement with its linear attenuation coefficient as its recorded high linear attenuation coefficient than *Triplochiton scleroxylon,* hence not the best suitable wood species to replace the wire mesh.

The conclusion of this work is that replacing the conventional wire mesh incorporated at the beam incident area with *Triplochiton scleroxylon* wood design of 2cm thickness on the EBRT couch top would be more affordable and effective.

5.2. RECOMMENDATION

From the findings of the linear attenuation coefficient and transmission characteristics of selected wood species the following recommendation are made:

5.2.1. NCRNM-KBTH

It is recommended that the findings of this study be used as a guideline for further studies on more wood species so that the wood species with best dosimetric properties selected to replace the wire mesh for some of the radiation treatment procedures, especially RT of prostate Ca involving five radiation fields at NCRNM-KBTH.

It is recommended that the depth and field size dependence on the TFs of the wooden couch top for radiation beam that traverses the couch top should be accounted for in the TPS at different treatment depth and field sizes associated with target volume localization in order to avoid dose discrepancies in the target volume with depth and field size.

NCRNM-KBTH should apply for authorization from the Nuclear Regulatory Authority when a decision is made to make the change from wire mesh table top couch to a wooden one.

5.2.2. Regulatory Body

The Nuclear Regulatory Authority should provide guidance for applying for authorization to replace the wire mesh with wood during the radiation treatment procedures at the NCRNM-KBTH when a decision is made to make that change.

5.2.3. Further studies

As it has been reported in most studies of the effect of beam modifiers such as wedges, bolus, compensators, collimator jaws, and blocks on skin dose for EBRT, it is therefore recommended that the effect of *Triplochiton scleroxylon* wood couch top on skin dose for EBRT be assessed prior to its use.

It is also recommended that more research on linear attenuation coefficient and transmission factor of more unexplored tropical woods to be conducted in order to compare the results to determine their suitability to replace very expensive carbon fibre couch top.

Finally, as the linear attenuation coefficient and transmission factor of carbon fiber for it's used in the fabrication of EBRT couch top were done using higher energy of radiation beam of 6MV, it is recommended that, the same study should be carried out with such energy range in order to compare the results with that of carbon fiber.

REFERENCES

[1]. Ravikumar M. and Ravichandran R., (2000) "Dose measurements in the build-up region for the photon beams from Clinac-1800 dual energy medical linear accelerator". Strahlentherapie and Onkologie, Vol. 176: 223-228.

[2]. Bentzen S.M., Heeren G., Cottier B., Slotman B., Glimelius B., Lievens Y., van den Bogaert W., (2005); "Towards evidence-based guidelines for radiotherapy infrastructure and staffing needs in Europe": the ESTRO QUARTS project. *Radiother Oncol*. 75(3): 355-65.

[3]. Dobbs J., Barrett A., Ash D., (1999), "Practical Radiotherapy Planning 3rd edition".

Oxford University Press New York

[4]. Washington C.M. and Leaver D.T., (2009), "Principles & Practice of Radiation Therapy -3rd edition". Mosby

[5]. Cember H., (1996); "Introduction to Health Physics- 3rd edition". McGraw-Hill Medical

[6]. Munjal R.K., Negi P.S., Babu A.G., Sinha S.N., Anand A.K., Kataria T., (2006); "Impact of 6MV photon beam attenuation by carbon fibre couch and immobilization devices in IMRT planning and dose delivery". J Med Phys. 31(2): 67–71.

[7]. McCormack S., Diffey J., Morgan A.M., (2005); "The effect of gantry angle on megavoltage photon beam attenuation by a carbon fiber couch insert". Med Phys.; 32(2):483–87.

[8]. Meara S.J, Langmack K.A., (1998); "An investigation into the use of carbon fibre for mega voltage radiotherapy applications". Phys Med Biol. 43(5):1359-1366.

[9]. de Mooy L.G., (1991); "The use of carbon fibres in radiotherapy". *Radiother Oncol*;

22(2): 40-42

[10]. Higgins D.M., Whitehurst P., Morgan A.M., (2001); "The effect of carbon fiber couch inserts on surface dose with beam size variations". Med Dosim 26: 251-254

[11]. Ernstberger T., Buchhorn G., Baums M.H., Heidrich G., (2007); "In-vitro MRI detectability of interbody test spacers made of carbon fibre-rein- forced polymers, titanium and titanium-coated carbon fibre-rein- forced polymers". *Acta Orthop Belg;* 73(2): 244-249.

[12]. Ding X.G., Duggan M.D., Lu B., Hallahan E.D., Cmelak A., Malcolm A., and Coffey W.C., (2007); "The Need for Accurate Dose Calculation Algorithms With Inhomogeneity Corrections in Treatment Planning for a Small Lung Tumor Treatment". *Int. J Radiat. Onc. Biol. and Phys*. 69, S697- S698.

[13]. Foster B.E., Wilson J., Badkul K.R., Kimler F.B., Smith M., Reddy K.E., and Wang F., (2009); "The Influence of Heterogeneity Dose Correction and Beam Energy on Planned Field Margins for Thoracic Tumors". *Int. J Radiat. Onc. Biol. and Phys*. 75, S622- S623

[14]. Plypoo A., Sethi A., Alsager S., Garza R., (2009); "Dose Correction Strategies for Inter-fraction Motion in Prostate IGRT". *Int. J Radiat. Onc. Biol. and Phys*. 75, S665- S666

[15]. Yaes R.J., (2001); "Late normal tissue injury from permanent interstitial implants". *Int. J of Radiat.Onc. Biol. and Phys.* 49, 1163 - 1169.

[16]. Hendee W.R., Ibbott G.S., (1996); "Radiation therapy physics". Mosby

[17]. William J.R., Thwaites D.I., (2001); "Radiotherapy physics I practice". Oxford University Press.

[18]. Almond P. R., Biggs P. J., Coursey B. M., Hanson W. F., Huq M. S., Math R., Rogers D. W. O., (1999), "AAPM's TG 51 Protocol for Clinical Reference Dosimetry of High-Energy Photon and Electron Beams", Med Phys. 26 (9); 1848 - 1860.

[19]. Khan F. M., (2010), "The Physics of Radiation Therapy", 4th Edition; 235-245

[20]. Lindquist, C., (1995); "Gamma knife radiosurgery, Semin". *Radiat. Oncol*. l5, 197 202.

[21].Walton, L., Bomford, C. K., and Ramsden, D., (1987); "The Sheffield stereotactic radiosurgery unit: Physical characteristics and principles of operation", *Br. J. Radiol*., 60, 897–906.

[22]. Leung P.M.K., Olch A.J., Rider W.D., Webb H.P., Aget H., John H.E., (1981); "Cobalt-60 therapy unit for large field irradiation", *Int. J. Radiat. Oncol*. Biol. Phys., 7, 705–771,

[23]. IAEA (International Atomic Energy Agency), (1998); "Design and implementation of a radiotherapy programme: Clinical, medical physics, radiation protection and safety aspects, TECDOC-1040, IAEA, Vienna". (Revision entitled Setting-up a radiotherapy programme: Clinical, medical physics, radiation protection and safety aspects, 2007.)

[24].Jones, D. E. A., Gregory, C., and Birchall, I., (1956); "Dosage distribution in rotational cobalt 60 therapy", *Br. J. Radiol*., 29,196–201.

[25]. Poffenbarger, B. A. and Podgorsak, E. B., (1998); "Viability of an isocentric cobalt60 teletherapy unit for stereotactic radiosurgery", Med. Phys., 25, 1935–1943.

[26].Warrington, A. P. and Adams, E. J., (2001); "Conformal and intensity modulated radiotherapy using cobalt-60 and 6 MV x-ray beams": A treatment planning comparison of different sites, *Radiother. Oncol*., 61(Suppl. 1), S73–S74.

[27]. Green D. T. and Errington, R. F., (1952); "Design of a cobalt 60 beam therapy unit", *Br. J. Radiol*., 25, 309–313,

[28]. John, H. E., Bates, L. M., and Watson, T. A., (1952); 1000 Curie cobalt units for radiation therapy", *Br. J. Radiol*., 25, 296–302,

[29]. Jaffray, D. A., Munro, P., and Battista, J. J., (1991); "Activity distribution of a cobalt60 teletherapy source", Med. Phys., 18, 288–291.

[30]. Podgorsak E. B., (2005), "Radiation Oncology Physics: A Handbook for Teachers and Students", Sponsored by IAEA; 161-271.

[31]. Mayles P., Nahum A., and Rosenwald J. C., (2007), "Handbook of Radiotherapy Physics": Theory and Practice", Published by Taylor and Francis Group, LLC; Vol. 12: 225-244.

[32].Theratron Equinox-100, External Beam Therapy System, User Manual, MDS Nordion, Canada

[33]. Poppe B, Chofor N, Rühmann A, Kunth W, Djouguela A, Kollhoff R et al., (2007); "The effect of a carbon-fibre couch on the depth-dose curves and transmission properties for megavoltage photon beams". Radiotherapy and Oncology Journal. 183(1): 43-48.

[34]. De Ost B., Vanregemorter J., Schaeken B., Van den Weyngaert D., (1997); "The effect of carbon fibre inserts on the build-up and attenuation of high energy photon beams". *Radiother Oncol*. 45(3): 275-277.

[35].Pulliam B.K., Howell M.R., Followill D., Luo D., White A.R. and Kry F.S., (2011); "The clinical impact of the couch top and rails on IMRT and arc therapy," Phys. Med. Biol. 56, 7435–7447

[36]. Vieira S.C., Kaatee R.S.J.P., Dirkx M.L.P., Heijmen B.J.M., (2003); "Two-dimensional measurement of photon beam attenuation by the treatment couch and immobilization devices using an electronic portal imaging device". Med Phys.:2981-2987.

[37]. Gillis S., Bral S., De Wagter C., Derie C., Paelinck L., Van Vaerenbergh K., (2005): "Evaluation of the Sinmed Mastercouch as replacement for a standard couch". *Radiother Oncol*, 75(2):227-236.

[38].Spezi E., Ferri A., (2007); "Dosimetric characteristics of the Siemens IGRT carbon fiber tabletop". Med Dosim, 32(4):295-298.

[39].Njeh C.F., Raines T.W., Saunders M.W., (2009); "Determination of the photon beam attenuation by the Brainlab imaging couch: angular and field size dependence". J Appl Clin Med Phys.

[40]. McCormack S., Diffey J., Morgan A., (2005); "The effect of gantry angle on megavoltage photon beam attenuation by a carbon fiber couch insert". *Med Phys, 32*(2):483-487.

[41]. Muthuswamy M.S., (1999); "A method of beam-couch intersection detection". Med Phys; 26(2):229-235.

[42]. Mihaylov I.B., Corry P., Yan Y., Ratanatharathorn V., Moros EG.,(2008); "Modelling of carbon fiber couch attenuation properties with a commercial treatment planning system". Med Phys. 35(11): 4982–4988.

[43]. Vanetti E., Nicolini G., Clivio A., Fogliata A., Cozzi L., (2009); "The impact of treatment couches modelling on RapidArc". Phys Med Biol.54 (9):N157–166.

[44] International Atomic Energy Agency (2006) Safety Report Series No. 47: Radiation protection in the design of Radiotherapy facilities. Vienna.

[45]. Olch A.J., Gerig L., Li H., Mihaylov I., Morgan A., (2014); "Dosimetric effects caused by couch tops and immobilization devices": Report of AAPM Task Group 176

[46]. Mondalek M.P., (1982); "Transmission and build up characteristics of polyurethane foam immobilization devices," Treat. Plann. **7**, 5–10.

[47]. Archambeau O.J., Pezner R., and Wasserman T., (1995); "Pathophysiology of irradiated skin and breast," *Int. J. Radiat. Oncol. Biol*., Phys. 31, 1171–1185.

[48]. Hoppe S.B., Laser B., Kowalski V.A., Fontenla C.S., Pena-Greenberg E., Yorke D.E., Lovelock M.D., Hunt A.M., and Rosenzweig E.K., (2008); "Acute skin toxicity

following stereotactic body radiation therapy for stage I nonsmall- cell lung cancer: who's at risk," *Int. J. Radiat. Oncol. Biol*., Phys. 72, 1283- 1286.

[49]. Kry F.S., Smith A.S., Weathers R., and Stovall M., (2012); "Skin dose during radiotherapy: a summary and general estimation technique," *J. Appl. Clin.* Med. Phys. 13, 20–34.

[50]. Meydanci T.P, Kemikler G., (2008); "Effect of a carbon fiber tabletop on the surface dose and attenuation for high-energy photon beams". Ra- diat Med. 26 (9): 539–544.

[51]. King C.S., Acker C.J., Kussin S.P.,Marks B.L., Weeks J.K. and Leopold A.K. (1996); "High-dose, hyper fractionated, accelerated radiotherapy using a concurrent boost for the treatment of nonsmall cell lung cancer: Unusual toxicity and promising early results*," Int. J. Radiat. Oncol. Biol*., Phys. 36, 593–599.

[52]. Krithivas G. and Rao N.S., (1988); "Arc therapy dose perturbation due to the center bar in a Clinac 4/100 couch assembly," Med. Dosim. 13, 15–18.

[53]. Sharma C.S., Johnson W.M., (1992); "Photon beam attenuation for a patient support assembly during arc therapy for a medical linear accelerator," Med. Dosim. 17, 225–228 (1992).

[54]. Myint W.K., Niedbala M., Wilkins D., Gerig L.H., (2006); "Investigating treatment dose error due to beam attenuation by a carbon fiber tabletop". J Appl Clin Med Phys 7(3):21-27.

[55]. Rajasekhar R and Kumar J.R.., (2014); "Experimental investigation of gamma radiation shielding characteristics of wood". Best. IJHAMS. Vol. 2; 21-26.

[56].Geyer P., Blank H., Zips D., and Alheit H., (2006); "Correction to BrainSCAN central axis dose calculations for 6-MV photon beams to lung with lateral electron disequilibrium". *Int. J Radiat. Onc. Biol. and Phys.* 66, S102-S107

[57]. Kaplan I., (1972); "Nuclear Physics (Addison-Wesley, New York)".

[58]. Opoku S.Y., Hanson J., Yarney J., Tagoe S.N.A., (2012): "Variation in Couch Transmission Factors with Treatment Depths in Isocentric Technique at the National

Radiotherapy Centre, Korle-Bu Teaching Hospital, Accra, Ghana". Science journal of medicine and clinical trials.sjmct-196.

.

APPENDICES

Appendix A

Raw data measurements of the transmitted beam showing average Temperature, Pressure and Corrected electrometer readings for determination of linear attenuation coefficient of the Wood species at different field size using SAD setup.

APPENDIX- A1: Treatment depth of 0.5cm

Table A 1: Wawa (*Triplochiton scleroxylon*)

Field size:5cm x 5cm						
	P1	P2	Av. Pressure/kpa			
	101.2	101.2	101.2	Average		
Thickness/cm	ERD1	ERD2	ERD3	ERD/nC	Tempt/^{o}C	Cor. ERD/nC
0 (open field)	4.327	4.3278	4.3288	4.327867	19.7	4.32771
2.5	4.0536	4.0544	4.0555	4.0545	19.7	4.054353
5	3.8331	3.8321	3.8319	3.832367	20	3.836154
7.5	3.5743	3.5784	3.5788	3.577167	20.3	3.584366
10	3.3588	3.3591	3.359	3.358967	20.3	3.365727
12.5	3.1451	3.1456	3.1464	3.1457	20.35	3.152568
15	2.9355	2.9362	2.9363	2.936	20.4	2.942911
Field size:10cm x 10cm						
	P1	P2	Av. Pressure/kpa			
	101.2	101.2	101.2	Average		
Thickness/cm	ERD1	ERD2	ERD3	ERD/nC	Tempt/^{0}C	Cor. ERD/nC
0 (open field)	4.5713	4.5728	4.573	4.572367	20.35	4.582349
2.5	4.2971	4.2969	4.2981`	4.297	20.9	4.314451
5	4.0663	4.0687	4.0703	4.068433	20.8	4.083567
7.5	3.8023	3.8052	4.806	4.137833	20.75	4.152519
10	3.5784	3.5786	3.5789	3.578633	20.7	3.590723
12.5	3.3549	3.3568	3.3576	3.356433	20.7	3.367773
15	3.1399	3.1421	3.1423	3.141433	20.55	3.150437

Continuation of Table A1

Field size: 15cm x 15cm						
	P1	P2	Av. Pressure/kpa			
	101.2	101.2	101.2	Average		
Thickness/cm	ERD1	ERD2	ERD3	ERD/nC	Tempt/^{o}C	Cor. ERD/nC
0 (open field)	4.7695	4.7723	4.772	4.771267	19.7	4.771094
2.5	4.5033	4.5015	4.5007	4.501833	19.7	4.50167
5	4.271	4.273	4.273	4.272333	19.7	4.272179
7.5	4.0095	4.0108	4.0094	4.0099	19.7	4.009755
10	3.7814	3.7795	3.782	3.780967	19.95	3.784057
12.5	3.5491	3.5509	3.5511	3.550367	20.2	3.5563
15	3.3306	3.3304	3.3315	3.330833	20.2	3.336399

Table A2: Danta *(Nesogogordonia papaverifera*)

Field size:5cm x 5cm						
	P1	P2	Av. Pressure/kpa			
	101.2	101.2	101.2	Average		
Thickness/cm	ERD1	ERD2	ERD3	ERD/nC	Tempt/^{o}C	Cor. ERD/nC
0 (open field)	4.327	4.3278	4.3288	4.327867	17.9	4.30111
2.5	3.8109	3.8139	3.8148	3.8132	18	3.790927
5	3.2589	3.2602	3.2613	3.260133	18	3.241091
7.5	2.8441	2.8447	2.8475	2.845433	18.05	2.829299
10	2.4228	2.4241	2.4244	2.423767	18.1	2.410437
12.5	2.0991	2.0998	2.1004	2.099767	18.1	2.088219
Field size:10cm x 10cm						
	P1	P2	Av. Pressure/kpa			
	101.2	101.2	101.2	Average		
Thickness/cm	ERD1	ERD2	ERD3	ERD/nC	Tempt/^{0}C	Cor. ERD/nC
0 (open field)	4.5713	4.5728	4.573	4.572367	17.9	4.544098
2.5	4.0591	4.0608	4.0614	4.060433	17.9	4.03533
5	3.491	3.4891	3.4908	3.4903	17.9	3.468721
7.5	3.0565	3.0584	3.0596	3.058167	18	3.040304
10	2.6175	2.618	2.6184	2.617967	18	2.602675
12.5	2.2749	2.2756	2.2721	2.2742	18.1	2.261693

Field size:15cm x 15cm						
	P1	P2	Av. Pressure/kpa			
	101.2	101.2	101.2	Average		
Thickness/cm	ERD1	ERD2	ERD3	ERD/nC	Tempt/^{o}C	Cor. ERD/nC
0	4.7695	4.7723	4.772	4.771267	17.9	4.741768
2.5	4.263	4.2648	4.2664	4.264733	18	4.239823
5	3.6925	3.6926	3.6938	3.692967	18.1	3.672657
7.5	3.2602	3.2608	3.2613	3.260767	18.1	3.242834
10	2.7989	2.8	2.7994	2.799433	18.1	2.784038
12.5	2.444	2.4424	2.4439	2.443433	18.1	2.429995

Table A3: Ofram (*Terminalia superba*)

Field size:5cm x 5cm						
	P1	P2	Av. Pressure/kpa			
	101.2	101.2	101.2	Average		
Thickness/cm	ERD1	ERD2	ERD3	ERD/nC	Tempt/^{o}C	Cor. ERD/nC
0	4.327	4.3278	4.3288	4.327867	17.8	4.299632
2.5	4.0506	4.0524	4.0525	4.051833	17.8	4.025399
5	3.7435	3.7436	3.7442	3.743767	17.8	3.719342
7.5	3.4348	3.436	3.437	3.435933	17.8	3.413517
10	3.1474	3.1487	3.1492	3.148433	17.8	3.127893
12.5	2.9039	2.9052	2.9047	2.9046	17.8	2.88565
15	2.6942	2.6949	2.6957	2.694933	17.8	2.677352
Field size:10cm x 10cm						
	P1	P2	Av. Pressure/kpa			
	101.2	101.2	101.2	Average		
Thickness/cm	ERD1	ERD2	ERD3	ERD/nC	Tempt/^{0}C	Cor. ERD/nC
0 (open field)	4.5713	4.5728	4.573	4.572367	17.9	4.544098
2.5	4.2952	4.2945	4.2953	4.295	18.1	4.271379
5	3.971	3.9729	3.9731	3.972333	18.05	3.949809
7.5	3.6599	3.6621	3.6634	3.6618	18.1	3.641662
10	3.3634	3.365	3.3658	3.364733	18	3.34508
12.5	3.1116	3.1124	3.1127	3.112233	17.9	3.092992
15	2.8911	2.8915	2.8911	2.891233	18	2.874346

Field size:15cm x1 5cm						
	P1	P2	Av. Pressure/kpa			
	101.2	101.2	101.2	Average		
Thickness/cm	ERD1	ERD2	ERD3	ERD/nC	Tempt/^{o}C	Cor. ERD/nC
0	4.7695	4.7723	4.772	4.771267	17.8	4.740139
2.5	4.4915	4.491	4.4907	4.491067	17.8	4.461767
5	4.1802	4.1824	4.1827	4.181767	17.8	4.154485
7.5	3.8628	3.8638	3.8643	3.863633	17.75	3.837767
10	3.5576	3.5586	3.5593	3.5585	17.7	3.534069
12.5	3.2954	3.2968	3.2969	3.296367	17.7	3.273736
15	3.071	3.0712	3.0716	3.071267	17.75	3.050705

Table A4: Cedar *(Entandrophragma Candollei)*

Field size:5cm x 5cm						
	P1	P2	Av. Pressure/kpa			
	101.2	101.2	101.2	Average		
Thickness/cm	ERD1	ERD2	ERD3	ERD/nC	Tempt/^{o}C	Cor. ERD/nC
0	4.327	4.3278	4.3288	4.327867	17.9	4.30111
2.5	3.9632	3.9607	3.9622	3.962033	17.95	3.938214
5	3.3951	3.3962	3.3977	3.396333	17.95	3.375915
7.5	3.0679	3.0701	3.0702	3.0694	18.05	3.051996
10	3.7836	2.7826	2.7818	3.116	18.05	3.098331
12.5	2.5216	2.5199	2.5222	2.521233	18.05	2.506937
15	2.2893	2.291	2.2909	2.2904	18.05	2.277413
Field size:10cm x 10cm						
	P1	P2	Av. Pressure/kpa			
	101.2	101.2	101.2	Average		
Thickness/cm	ERD1	ERD2	ERD3	.ERD/nC	Tempt/^{o}C	Cor. ERD/nC
0 (open field)	4.5713	4.57 28	4.573	4.572367	18	4.545659
2.5	4.2089	4.2093	4.2101	4.209433	18	4.184846
5	3.6256	3.6266	3.6272	3.626467	17.9	3.604046
7.5	3.2899	3.2921	3.2924	3.291467	17.95	3.271679
10	2.993	2.994	2.9957	2.994233	18.05	2.977255
12.5	2.7142	2.7148	2.7163	2.7151	17.95	2.698777
15	2.4675	2.4686	2.4705	2.468867	18.1	2.455289

Field size:15cm x 15cm						
	P1	P2	Av. Pressure/kpa			
	101.2	101.2	101.2	Average		
Thickness/cm	ERD1	ERD2	ERD3	ERD/nC	Tempt/^{o}C	Cor. ERD/nC
0	4.7695	4.7723	4.772	4.771267	18.15	4.745841
2.5	4.4133	4.4126	4.4105	4.412133	18.1	4.387868
5	3.8291	3.8305	3.8323	3.830633	17.9	3.80695
7.5	3.4905	3.4918	3.4916	3.4913	17.9	3.469715
10	3.1876	3.1901	3.1909	3.189533	18.05	3.171448
12.5	2.8984	2.8987	2.9003	2.899133	18	2.882199
15	2.6416	2.6435	2.6448	2.6433	18.1	2.628763

Table A5: Okoro (*Albizia zygia*)

Field size:5cm x 5cm						
	P1	P2	Av. Pressure/kpa			
	101.2	101.2	101.2	Average		
Thickness/cm	ERD1	ERD2	ERD3	ERD/nC	Tempt/^{o}C	Cor. ERD/nC
0 (open field)	4.327	4.3278	4.3288	4.327867	18.1	4.304065
2.5	3.9591	3.9599	3.9617	3.960233	18.1	3.938454
5	3.6492	3.6504	3.651	3.6502	18.1	3.630125
7.5	3.2589	3.2561	3.2576	3.257533	18.1	3.239618
10	3.0087	3.0104	3.0113	3.010133	18.1	2.993579
12.5	2.7506	2.7488	2.75	2.7498	18	2.733738
15	2.4881	2.4896	2.4906	2.489433	17.9	2.474042
Field size:10cm x 10cm						
	P1	P2	Av. Pressure/kpa			
	101.2	101.2	101.2	Average		
Thickness/cm	ERD1	ERD2	ERD3	.ERD/nC	Tempt/^{0}C	Cor. ERD/nC
0 (open field)	4.5713	4.5728	4.573	4.572367	17.9	4.544098
2.5	4.2071	4.208	4.2091	4.208067	18	4.183487
5	3.8981	3.8998	3.9003	3.8994	18	3.876623
7.5	3.5049	3.5053	3.5063	3.5055	17.9	3.483827
10	3.241	3.2425	3.2427	3.242067	17.9	3.222023
12.5	2.97	2.9706	2.9706	2.9704	17.9	2.952035
15	2.6953	2.6961	2.6983	2.696567	17.9	2.679895

Field size:15cm x 15cm						
	P1	P2	Av. Pressure/kpa			
	101.2	101.2	101.2	Average		
Thickness/cm	ERD1	ERD2	ERD3	ERD/nC	Tempt/^{o}C	Cor. ERD/nC
0 (open field)	4.7695	4.7723	4.772	4.771267	17.7	4.73851
2.5	4.4204	4.4212	4.4213	4.420967	17.8	4.392124
5	4.1129	4.1139	4.115	4.113933	17.9	4.088499
7.5	3.7112	3.7122	3.713	3.712133	17.9	3.689183
10	3.4417	3.4414	3.4411	3.4414	17.9	3.420124
12.5	3.1584	3.1589	3.1601	3.159133	17.95	3.140141
15	2.8809	2.8812	2.8819	2.881333	17.95	2.864011

APPENDIX- A2: Treatment depth of 5cm

Table A6: Wawa (*Triplochiton scleroxylon*)

Field size: 5cm x 5ccm						
	P1	P2	Av.Pressure/kpa			
	101.2	101.2	101.2	Average		
Thickness/cm	ERD1	ERD2	ERD3	ERD/nC	Tempt/nC	Cor.Av.ERD/nC
0 (open field)	3.6499	3.6591	3.6604	3.656467	19.1	3.648843
2.5	3.3963	3.4064	3.4083	3.403667	19.1	3.39657
5	3.1424	3.1487	3.1504	3.147167	19.1	3.140605
7.5	2.9505	2.9552	2.9551	2.9536	19.1	2.947442
10	2.7642	2.771	2.7726	2.769267	19.1	2.763493
12.5	2.5996	2.6065	2.607	2.604367	19.1	2.598937
15	2.4202	2.4264	2.4282	2.424933	19.1	2.419877
Field size: 10cm x 10cm						
	P1	P2	Av.Pressure/kpa			
	101.2	101.2	101.2	Average		
Thickness/cm	ERD1	ERD2	ERD3	ERD/nC	Tempt/^{0}C	Cor.Av.ERD/nC
0 (open field)	4.0152	4.0227	4.024	4.020633	19.1	4.01225
2.5	3.7852	3.7869	3.7884	3.786833	19.1	3.778938
5	3.581	3.5821	3.5826	3.5819	19.05	3.57382
7.5	3.354	3.3551	3.3553	3.3548	19.05	3.347233
10	3.1627	3.1628	3.1638	3.1631	19	3.155425
12.5	2.9638	2.9643	2.9645	2.9642	18.9	2.955995
15	2.7718	2.7722	2.7723	2.7721	18.9	2.764427
Field size:15cm x 15cm						
	P1	P2	Av.Pressure/kpa			
	101.2	101.2	101.2	Average		
Thickness/cm	ERD1	ERD2	ERD3	ERD/nC	Tempt/nC	Cor.Av.ERD/nC
0 (open field)	4.2857	4.2867	4.2887	4.287033	18.95	4.275899
2.5	4.0338	4.034	4.0341	4.033967	18.9	4.022801
5	3.8255	3.827	3.8277	3.826733	18.9	3.816141
7.5	3.5924	3.5901	3.5916	3.591367	18.9	3.581426
10	3.3916	3.3929	3.3926	3.392367	19	3.384135
12.5	3.189	3.1892	3.1899	3.189367	18.95	3.181083
15	2.9845	2.9852	2.9859	2.9852	18.9	2.976937

Table A7: Danta (*Nesogogordonia papaverifera*)

Field size: 5cm x 5ccm						
	P1	P2	Av.Pressure/kpa			
	101.2	101.2	101.2	Average		
Thickness/cm	ERD1	ERD2	ERD3	ERD/nC	Tempt/^{0}C	Cor.Av.ERD/nC
0 (open field)	3.6499	3.6591	3.6604	3.656467	18.8	3.645097
2.5	3.1278	3.1361	3.1392	3.134367	18.8	3.124621
5	2.6626	2.6692	2.6715	2.667767	18.8	2.659472
7.5	2.2531	2.2672	2.2662	2.262167	18.85	2.255519
10	1.9839	1.986	1.9858	1.985233	18.9	1.979738
12.5	1.6954	1.6994	1.701	1.6986	18.85	1.693608
Field size: 10cm x 10cm						
	P1	P2	Av.Pressure/kpa			
	101.2	101.2	101.2	Average		
Thickness/cm	ERD1	ERD2	ERD3	ERD/nC	Tempt/nC	Cor.Av.ERD/nC
0 (open field)	4.0152	4.0227	4.024	4.020633	18.8	4.008132
2.5	3.4973	3.4968	3.4968	3.496967	18.8	3.486093
5	2.9948	2.9956	2.9963	2.995567	18.8	2.986252
7.5	2.6348	2.6341	2.6321	2.633667	18.8	2.625478
10	2.2621	2.2628	2.2632	2.2627	18.8	2.255664
12.5	1.9824	1.9821	1.9827	1.9824	18.85	1.976574
Field size:15cm x 15cm						
	P1	P2	Av.Pressure/kpa			
	101.2	101.2	101.2	Average		
Thickness/cm	ERD1	ERD2	ERD3	ERD/nC	Tempt/nC	Cor.Av.ERD/nC
0 (open field)	4.2857	4.2867	4.2887	4.287033	18.85	4.274435
2.5	3.7381	3.739	3.7403	3.739133	18.85	3.728145
5	3.2268	3.2278	3.2279	3.2275	18.85	3.218016
7.5	2.8561	2.8554	2.8566	2.856033	18.9	2.848128
10	2.4666	2.4669	2.4679	2.467133	18.9	2.460305
12.5	2.1712	2.172	2.1723	2.171833	18.85	2.165451

Table A8: Ofram (*Terminalia superba*)

Field size: 5cm x 5ccm						
	P1	P2	Av.Pressure/kpa			
	101.2	101.2	101.2	Average		
Thickness/cm	ERD1	ERD2	ERD3	ERD/nC	Tempt/^{0}C	Cor.Av.ERD/nC
0 (open field)	3.6499	3.6591	3.6604	3.656467	19.3	3.65134
2.5	3.3677	3.383	3.384	3.378233	19.3	3.373497
5	3.1237	3.1299	3.1313	3.1283	19.3	3.123914
7.5	2.865	2.8703	2.8716	2.868967	19.25	2.864454
10	2.6509	2.6593	2.6605	2.6569	19.2	2.652268
12.5	2.433	2.4377	2.4375	2.436067	19.15	2.431403
15	2.2424	2.2479	2.2496	2.246633	19.1	2.241949
Field size: 10cm x 10cm						
	P1	P2	Av.Pressure/kpa			
	101.2	101.2	101.2	Average		
Thickness/cm	ERD1	ERD2	ERD3	.ERD/nC	tempt/^{O}C	Cor.Av.ERD/nC
0 (open field)	4.0152	4.0227	4.024	4.020633	19.3	4.014996
2.5	3.7369	3.7382	3.7392	3.7381	19.3	3.732859
5	3.4419	3.4417	3.4408	3.441467	19.3	3.436641
7.5	3.1711	3.1716	3.1722	3.171633	19.2	3.166103
10	2.9424	2.9417	2.9405	2.941533	19.1	2.9354
12.5	2.7411	2.7418	2.7407	2.7412	19.1	2.735485
15	2.5247	2.5242	2.5284	2.525767	19.1	2.5205
Field size:15cm x 15cm						
	P1	P2	Av.Pressure/kpa			
	101.2	101.2	101.2	Average		
Thickness/cm	ERD1	ERD2	ERD3	ERD/nC	tempt/^{0}C	Cor.Av.ERD/nC
0 (open field)	4.2857	4.2867	4.2887	4.287033	18.9	4.275167
2.5	3.9879	3.9878	3.9885	3.988067	18.9	3.977028
5	3.6859	3.685	3.6868	3.6859	18.95	3.676327
7.5	3.4049	3.4057	6.4061	4.405567	19	4.394877
10	3.1673	3.1676	3.1687	3.167867	19.05	3.160721
12.5	2.9575	2.9526	2.9588	2.9563	19.1	2.950136

Table A9: Cedar Kokote (*Entandrophragma candollei*)

Field size: 5cm x 5ccm						
	P1	P2	Av.Pressure/kpa			
	101.2	101.2	101.2	Average		
Thickness/cm	ERD1	ERD2	ERD3	ERD/nC	tempt/^{0}C	Cor.Av.ERD/nC
0 (open field)	3.6499	3.6591	3.6604	3.656467	19.1	3.648843
2.5	3.3076	3.3163	3.3163	3.3134	19.1	3.306492
5	3.0052	3.0122	3.0134	3.010267	19.1	3.00399
7.5	2.7227	2.73	2.7309	2.727867	19.1	2.722179
10	2.4766	2.486	2.4842	2.482267	19.1	2.477091
12.5	2.2425	2.2522	2.2525	2.249067	19.1	2.244377
Field size: 10cm x 10cm						
	P1	P2	Av.Pressure/kpa			
	101.2	101.2	101.2	Average		
Thickness/cm	ERD1	ERD2	ERD3	ERD/nC	Tempt/^{0}C	Cor.Av.ERD/nC
0 (open field)	4.0152	4.0227	4.024	4.020633	19.1	4.01225
2.5	3.6789	3.6783	3.6791	3.678767	19.1	3.671096
5	3.3392	3.3406	3.3403	3.340033	19.1	3.333069
7.5	2.8772	2.8779	2.8794	2.878167	19.1	2.872166
10	2.6137	2.6136	2.6125	2.613267	19.1	2.607818
12.5	2.3827	2.3814	2.3836	2.382567	19.2	2.378413
15	2.17	2.1703	2.1706	2.1703	19.2	2.166516
Field size:15cm x 15cm						
	P1	P2	Av.Pressure/kpa			
	101.2	101.2	101.2	Average		
Thickness/cm	ERD1	ERD2	ERD3	ERD/nC	tempt/^{0}C	Cor.Av.ERD/nC
0 (open field)	4.2857	4.2867	4.2887	4.287033	19.1	4.278095
2.5	3.9217	3.9237	3.9232	3.922867	19.1	3.914688
5	3.5828	3.582	3.5833	3.5827	19.2	3.576453
7.5	3.1038	3.1045	3.103	3.103767	19.15	3.097825
10	3.8287	2.8306	2.8307	3.163333	19.1	3.156738
12.5	3.5876	2.5885	2.5883	2.921467	19.2	2.916373
15	2.3607	2.3611	2.3617	2.361167	19.1	2.356244

Table A10: Okoro (*Albizia zygia*)

Field size:5cm x 5cm						
	P1	P2	Av.Pressure/kpa			
	101.2	101.2	101.2	Average		
Thickness/cm	ERD1	ERD2	ERD3	ERD/nC	.Tempt/^{o}C	Cor.ERD/nC
0 (open field)	3.6499	3.6591	3.6604	3.656467	18.9	3.646346
2.5	3.2658	3.2741	3.2763	3.272067	18.9	3.26301
5	2.9222	2.9365	2.9365	2.931733	18.95	2.924119
7.5	2.6511	2.6555	2.6612	2.655933	19	2.649489
10	2.4163	2.421	2.4229	2.420067	18.9	2.413368
12.5	2.2086	2.2241	2.2247	2.219133	18.8	2.212233
15	1.9677	1.9736	1.974	1.971767	18.85	1.965972
Field size:10cm x 10cm						
	P1	P2	Av.Pressure/kpa			
	101.2	101.2	101.2	Average		
Thickness/cm	ERD1	ERD2	ERD3	ERD/nC	Tempt/^{o}C	Cor.ERD/nC
0 (open field)	4.0152	4.0227	4.024	4.020633	18.8	4.008132
2.5	3.7381	3.7389	3.7399	3.738967	18.8	3.727341
5	3.3543	3.3551	3.3554	3.354933	18.8	3.344502
7.5	3.0955	3.0966	3.097	3.096367	18.8	3.086739
10	2.8342	2.8353	2.8361	2.8352	18.85	2.826868
12.5	2.5762	2.575	2.5777	2.5763	18.85	2.568729
15	2.322	2.3223	2.3215	2.321933	18.85	2.31511
Field size:15cm x 15cm						
	P1	P2	Av.Pressure/kpa			
	101.2	101.2	101.2	Average		
Thickness/cm	ERD1	ERD2	ERD3	ERD/nC	Tempt/^{O}C	Cor.ERD/nC
0 (open field)	4.2857	4.2867	4.2887	4.287033	19	4.276631
2.5	3.9843	3.9836	3.986	3.984633	18.95	3.974285
5	3.5922	3.5927	3.5923	3.5924	18.9	3.582457
7.5	3.3263	3.3268	3.3274	3.326833	18.9	3.317625
10	3.0564	3.0572	3.0572	3.05693	18.85	3.04795
12.5	2.7893	2.7902	2.79	2.78983	18.85	2.78164
15	2.522	2.5229	2.5225	2.52247	18.95	2.51592

APPENDIX B

Calculated $I_n\,(Cor.Av.electrometer\ readings/TB)$ as a function of thickness of wood species for different field sizes at a depth of 0.5cm used for the study

Table B. 1: Wawa (*Triplochiton scleroxylon*)

	In(Cor.Av.electrometer readings/TB)		
Thickness /cm	**5cm x 5cm**	**10cm x 10cm**	**15cm x 15cm**
0	1.46504	1.52221	1.56258
2.5	1.39979	1.46197	1.50445
5	1.34447	1.40697	1.45212
7.5	1.27658	1.42372	1.38873
10	1.21364	1.27835	1.3308
12.5	1.14822	1.21425	1.26872
15	1.0794	1.14754	1.20489
	Appendix B2: Danta (*Nesogogordonia papaverifera*)		
0	1.45887	1.51383	1.55641
2.5	1.33261	1.39509	1.44452
5	1.17591	1.24379	1.30092
7.5	1.04003	1.11196	1.17645
10	0.87981	0.95654	1.0239
12.5	0.73631	0.81611	0.88789
	Appendix B3: Ofram (*Terminalia superba*)		
0	1.45853	1.51383	1.55607
2.5	1.39262	1.45194	1.49555
5	1.31355	1.37367	1.42419
7.5	1.22774	1.29244	1.34489
10	1.14036	1.20749	1.26245
12.5	1.05975	1.12914	1.18593
15	0.98483	1.05583	1.11537

Table B.4: Cedar kokote (*Entandrophragma candollei*)

	In(Cor.Av.electrometer readings)		
Thickness /cm	**5cm x 5cm**	**10cm x 10cm**	**15cm x 15cm**
0	1.45887	1.51417	1.55727
2.5	1.37073	1.43147	1.47884
5	1.21667	1.28206	1.33683
7.5	1.1158	1.1853	1.24407
10	1.13086	1.091	1.15419
12.5	0.91906	0.9928	1.05855
15	0.82304	0.89824	0.96651
	Table- B.5: Okoro(*Albizia zygia*)		
0	1.45956	1.51383	1.55572
2.5	1.37079	1.43115	1.47981
5	1.28927	1.35496	1.40818
7.5	1.17546	1.24813	1.30541
10	1.09647	1.17001	1.22968
12.5	1.00567	1.0825	1.14427
15	0.90585	0.98578	1.05222

APPENDIX C

Calculated I_n $(Cor.Av.electrometer\ readings/TB)$ as a function of thickness of wood species for different field sizes at a depth of 5cm used for the study

Table C. 1: Wawa (*Triplochiton scleroxylon*)

	In(Cor.Av.electrometer reading)/nC		
Thickness/cm	**5cm x 5cm**	**10cm x 10cm**	**15cm x 15cm**
0	1.29441	1.38935	1.45299
2.5	1.22277	1.32944	1.39198
5	1.14442	1.27364	1.33924
7.5	1.08094	1.20813	1.27576
10	1.0165	1.14912	1.2191
12.5	0.9551	1.08384	1.15722
15	0.88372	1.01683	1.0909
	Table- C.2:Danta *(Nesogogordonia papaverifera*)		
0	1.29338	1.38833	1.45265
2.5	1.13931	1.24878	1.31591
5	0.97813	1.09402	1.16877
7.5	0.81338	0.96526	1.04666
10	0.68297	0.81344	0.90029
12.5	0.52686	0.68137	0.77263
	Table- C.3:Ofram (*Terminalia superba*)		
0	1.29509	1.39004	1.45282
2.5	1.21595	1.31717	1.38054
5	1.13909	1.2345	1.30191
7.5	1.05238	1.1525	1.48044
10	0.97542	1.07684	1.1508
12.5	0.88847	1.00631	1.08185
15	0.80735	0.92446	1.0025

Table C.4: Cedar kokote (*Entandrophragma candollei*)

	In(Cor.Av.electrometer reading)/nC		
Thickness/cm	**5cm x 5cm**	**10cm x 10cm**	**15cm x 15cm**
0	1.29441	1.38935	1.45351
2.5	1.19589	1.30049	1.36474
5	1.09994	1.20389	1.27437
7.5	1.00143	1.05507	1.1307
10	0.90709	0.95851	1.14954
12.5	0.80843	0.86643	1.07034
		0.77312	0.85707
	Table- C.5:Okoro (*Albizia zygia*)		
0	1.29373	1.38833	1.45317
2.5	1.18265	1.3157	1.37985
5	1.07299	1.20732	1.27605
7.5	0.97437	1.12712	1.19925
10	0.88102	1.03917	1.11447
12.5	0.794	0.94341	1.02304
15	0.67599	0.83946	0.92264

APPENDIX D

Raw data measurements showing average Temperature, Pressure and Corrected ion chamber readings for Wood species TF at different Fs and depths using SAD setup.

Table D. 1: Treatment depth of 0.5cm

Open field								
		P1	P2	Av. Pressure/kpa				
		101.1	101.1	101.1				
Field size/cm	ERD1	ERD2	ERD3	Av.ERD/nC	T1	T2	Av. Tempt/^{o}C	Cor. ERD/nC
5 x 5	4.4634	4.4612	4.4604	4.461667	19.1	19.1	19.1	4.456768
10 x 10	4.7077	4.7093	4.7181	4.7117	19.1	19.1	19.1	4.706527
15 x 15	4.9058	4.9143	4.9114	4.9105	19.1	19.2	19.15	4.905948
Wawa *(Triplochiton scleroxylon)*								
		P1	P2	Av. Pressure/kpa				
		101.1	101.1	101.1				
Field size/cm	ERD1	ERD2	ERD3	Av.ERD/nC	T1	T2	Av. Tempt/^{O}C	Cor. ERD/nC
5 x 5	4.3443	4.3532	4.3555	4.351	19.1	19.1	19.1	4.346223
10 x 10	4.6119	4.6206	4.6231	4.618533	19.1	19.1	19.1	4.613462
15 x 15	4.8128	4.8235	4.8253	4.820533	19.1	19.2	19.15	4.816065
Danta (*Nesogogordonia papaverifera*)								
			P1	P2	Av.Pressure/kpa			
			101.1	101.1	101.1			
Field size/cm	ERD1	ERD2	ERD3	Av.ERD/nC	T1	T2	Av. Tempt/^{o}C	cor. ERD/nC
5 x 5	4.1665	4.1759	4.1784	4.1736	19	19.1	19.05	4.168304
10 x 10	4.4774	4.4854	4.4875	4.483433	19.1	19	19.05	4.477745
15 x 15	4.6874	4.6994	4.7026	4.696467	19.1	19.2	19.15	4.692113
Ofram (*Terminalia superba*)								
			P1	P2	Av. Pressure/kpa			
			101.1	101.1	101.1			
Field size/cm	ERD1	ERD2	ERD3	Av.ERD/nC	T1	T2	Av. Tempt/^{o}C	cor. ERD/nC
5 x 5	4.3537	4.3616	4.3627	4.359333	19	19.1	19.05	4.353802
10 x 10	4.6242	4.634	4.6365	4.631567	19.1	18.9	19	4.624898
15 x 15	4.8204	4.8317	4.8342	4.828767	18.9	18.9	18.9	4.820164

Cedar kokote (*Entandrophragma candollei*)								
			P1	P2	Av. Pressure/kpa			
			101.1	101.1	101.1			
Field size/cm	ERD1	ERD2	ERD3	Av.ERD/nC	T1	T2	Av. Tempt/^{o}C	cor. ERD/nC
5 x 5	4.2957	4.3065	4.3098	4.304	19.2	19.1	19.15	4.30001
10 x 10	4.5832	4.5914	4.5923	4.588967	19.1	19.1	19.1	4.583928
15 x 15	4.7912	4.8017	4.8026	4.7985	19.1	19.2	19.15	4.794052
Okoro *(Albizia zygia*)								
			P1	P2	Av. Pressure/kpa			
			101.1	101.1	101.1			
Field size/cm	ERD1	ERD2	ERD3	Av.ERD/nC	T1	T2	Av. Tempt/^{o}C	cor. ERD/nC
5 x 5	4.2621	4.2717	4.2742	4.269333	19.1	19.1	19.1	4.264646
10 x 10	4.5622	4.5639	4.5577	4.561267	19.1	19.2	19.15	4.557038
15 x 15	4.7506	4.7607	4.7626	4.757967	19.2	19	19.1	4.752743

Table D. 2: Treatment depth of 5cm

Open field								
	P1	P2	Av.Pressure/kpa					
	101.1	101.1	101.1					
Field size/cm^2	ERD1	ERD2	ERD3	Av.ERD/nC	T1	T2	Av.Tempt/^{O}C	Cor.ERD/nC
5 x 5	3.6359	3.6451	3.6468	3.6426	19.6	19.6	19.6	3.644826
10 x 10	4.0265	4.0336	4.0345	4.031533	19.6	19.6	19.6	4.033997
15 x 15	4.2765	4.2897	4.2885	4.2849	19.6	19.6	19.6	4.287518
Wawa *(Triplochiton scleroxylon*)								
	P1	P2	Av.Pressure/kpa					
	101.1	101.1	101.1					
Field size/cm^2	ERD1	ERD2	ERD3	Av.ERD/nC	T1	T2	Av.Tempt/^{O}C	Cor. ERD/nC
5 x 5	3.4097	3.4171	3.4184	3.415067	19.6	19.6	19.6	3.417153
10 x 10	3.8189	3.8274	3.8292	3.825167	19.5	19.6	19.55	3.82685
15 x 15	4.0818	4.0911	4.0926	4.0885	19.6	19.5	19.55	4.0903
Danta *(Nesogogordonia papaverifera*)								
		P1	P2	Av. Pressures/kpa				
		101.1	101.1	101.1				
Field size/cm^2	ERD1	ERD2	ERD3	Av. ERD/nC	T1	T2	Av. Tempt/^{O}C	Cor.ERD/nC
5 x 5	3.1746	3.1837	3.1843	3.180867	19.5	19.5	19.5	3.181723
10 x 10	3.6165	3.621	3.6229	3.620133	19.5	19.3	19.4	3.619871
15 x 15	3.8961	3.9037	3.9059	3.9019	19.3	19.3	19.3	3.900283
Ofram *(Terminalia superba)*								
		P1	P2	Av. Pressure/kpa				
		101.1	101.1	101.1				
Field size/cm^2	ERD1	ERD2	ERD3	Av.ERD/nC	T1	T2	Av. Tempt/^{O}C	Cor. ERD/nC
5 x 5	3.431	3.437	3.4387	3.435567	19.3	19.3	19.3	3.434143
10 x 10	3.8414	3.8493	3.8499	3.846867	19.3	19.3	19.3	3.845273
15 x 15	4.1066	4.1179	4.1191	4.114533	19.3	19.3	19.3	4.112829

Cedar kokote (*Entandrophragma candollei*)								
		P1	P2	Av.Pressure/kpa				
		101.1	101.1	101.1				
Field size/cm^2	ERD1	ERD2	ERD3	Av.ERD/nC	T1	T2	Av.Tempt/C	Cor. ERD/nC
5 x 5	3.3653	3.3713	3.3728	3.3698	19.4	19.4	19.4	3.369556
10 x 10	3.7837	3.7903	3.7912	3.7884	19.4	19.3	19.35	3.787478
15 x 15	4.056	4.0645	4.0654	4.061967	19.3	19.3	19.3	4.060284
Okoro *(Albizia zygia)*								
		P1	P2	Av.Pressure/kpa				
		101.1	101.1	101.1				
Field size/cm^2	ERD1	ERD2	ERD3	Av.ERD/nC	T1	T2	Av.Tempt/^{O}C	Cor.ERD/nC
5 x 5	3.2963	3.3046	3.3051	3.302	19.6	19.6	19.6	3.304018
10 x 10	3.7178	3.7252	3.7247	3.722567	19.6	19.6	19.6	3.724841
15 x 15	3.9934	4.0038	4.0047	4.000633	19.6	19.6	19.6	4.003078

APPENDIX E.

Wood TFs at various field sizes for different wood species obtained from measurements at the two stipulated treatment depths using the SAD set-up.

Table E. 1: Treatment depth of 0.5cm

	Corrected Average electrometer readings/nC					
Field size/cm	**Open field**	**Wawa**	**Danta**	**Ofram**	**Cedar kokote**	**Okoro**
5 x 5	4.456768	4.346223	4.168304	4.353802	4.30001	4.264646
10 x 10	4.706527	4.613462	4.477745	4.624898	4.583928	4.557038
15 x 15	4.905948	4.816065	4.692113	4.820164	4.794052	4.752743
Transmission Factor						
5 x 5	1	0.975196	0.935275	0.976897	0.964827	0.956892
10 x 10	1	0.980226	0.95139	0.982656	0.973951	0.968238
15 x 15	1	0.981679	0.956413	0.982514	0.977192	0.968772
Mean	1	0.979	0.948	0.981	0.972	0.965
St.dev.	0	0.003	0.011	0.003	0.006	0.007

Table E.2: Treatment depth of 5cm

	Corrected Average electrometer readings/nC					
Field size/cm	**Open field**	**Wawa**	**Danta**	**Ofram**	**Cedar kokote**	**Okoro**
5cm x 5cm	3.644826	3.417153	3.181723	3.434143	3.369556	3.304018
10cm x 10cm	4.033997	3.82685	3.619871	3.845273	3.787478	3.724841
15cm x 15cm	4.287518	4.0903	3.900283	4.112829	4.060284	4.003078
Transmission Factor						
5cm x5cm	1	0.937535	0.872942	0.942197	0.924477	0.906495
10cm x10cm	1	0.94865	0.897341	0.953217	0.93889	0.923362
15cm x 15cm	1	0.954002	0.909683	0.959256	0.947001	0.933659
Mean	1	0.947	0.893	0.952	0.938	0.921
St dev.	0	0.008	0.019	0.009	0.011	0.014